ACS SENSORS

pubs.acs.org/acssensors

Review

Magnetoelastic Resonance Sensors: Principles, Applications, and Perspectives

Paula G. Saiz,* Roberto Fernández de Luis, Andoni Lasheras, María Isabel Arriortua, and Ana Catarina Lopes

Cite This: https://doi.org/10.1021/acssensors.2c00032

Read Online

ACCESS | Metrics & More | Article Recommendations

ABSTRACT: Magnetoelastic resonators are gaining attention as an incredibly versatile and sensitive transduction platform for the detection of varied physical, chemical, and biological parameters. These sensors, based on the coupling effect between mechanical and magnetic properties of ME platforms, stand out in comparison to alternative technologies due to their low cost and wireless detection capability. Several parameters have been optimized over the years to improve their performance, such as their composition, surface functionalization, or shape geometry. In this review, the working principles, recent advances, and future perspectives of magnetoelastic resonance transducers are introduced, highlighting their potentials as a versatile platform for sensing applications. First, the fundamental principles governing the magnetoelastic resonators performance are introduced as well as the most common magnetoelastic materials and their main fabrication methods are described. Second, the versatility and technical feasibility of magnetoelastic resonators for biological, chemical, and physical sensing are highlighted and the most recent results and functionalization processes are summarized. Finally, the forefront advances to further improve the performance of magnetoelastic resonators for sensing applications have been identified.

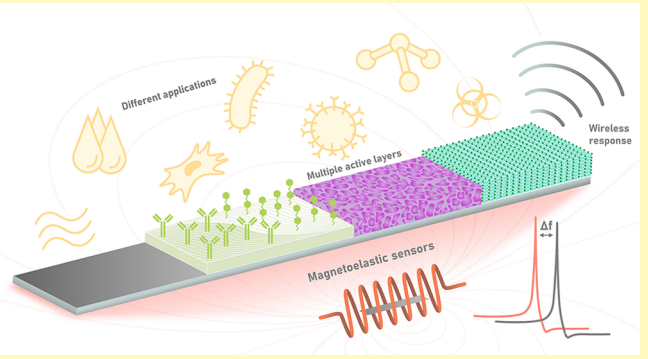

KEYWORDS: *chemical sensors, biosensors, wireless detection, magnetoelastic resonance, geometry engineering, magnetoelastic alloys, advanced functionalization, high sensitivity devices*

Transducers are able to translate a given energy input into an easily readable and measurable output signal, and henceforth, they are classified in function of the energy transformation type performed.[1] Electroacoustic, piezoelectric, or electrochemical/physical/optical transduction processes are found in many devices of our day-by-day life. The evolution of novel transduction systems is a cornerstone to combine high accuracy with a cheap, quick, repetitive, highly sensitive, and selective detection. Once evolved and improved, transducers will play a key role in developing sensor technologies for the 4.0 industrialization or advanced environmental monitoring systems.[2−6] In addition, there is no need to mention the key role that biological sensors played to, for example, monitor and control the COVID-19 pandemic.[7−9] Nevertheless, wireless sensing is only accessible for some of the transduction technologies reported at the present time. Here is where magnetoelastic systems exhibit intrinsic advantages in comparison to alternative technologies.

In that respect, magnetoelastic (ME) acoustic wave (AW) type transducers are gaining attention within the scientific community because, in addition to their fast response, low cost, and high sensitivity, they perform the transduction and sensing process wirelessly.[10−12] In contrast, other AW technologies, such as quartz crystal microbalance (QCM) or microcantilevers (MCL), lack wireless detection capability, which limits their application range.[13,14]

The AW-based detection process relies on the variations of the properties of the acoustic waves traveling through the sensor when exposed to different perturbations. In the case of ME materials, a marked magnetoelastic resonance frequency is displayed when it is under an alternating magnetic field. This resonance frequency varies when the material is exposed to such perturbations. So, ME AW transducers themselves are able to measure physical parameters such as mass loadings or viscosity changes without the need of further modifications.[15] In addition, the surface of the magnetoelastic resonator can be functionalized to recognize specific targets (i.e., chemical or

Received: January 5, 2022
Accepted: April 8, 2022

© XXXX American Chemical Society

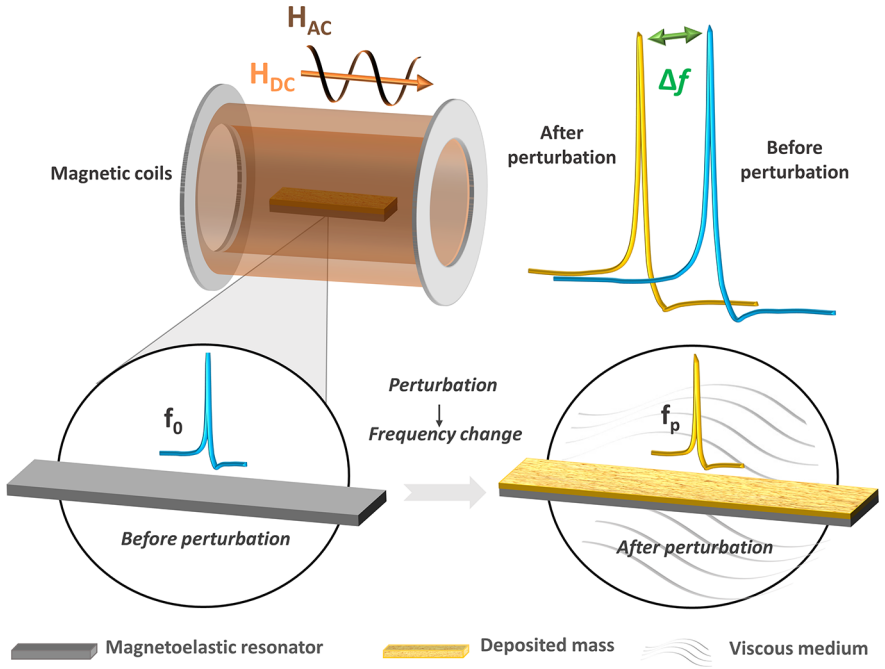

Figure 1. Scheme of a magnetoelastic sensor working principle.

biological), which lead to a magnified surface perturbation (i.e., mass gain) when the chemical or biological pathogen interacts with the functionalized active layer of the systems. So, generally speaking, magnetoelastic resonance sensor research is commonly based on two main challenges: (i) the improvement of the magnetoelastic resonators response itself and (ii) the surface functionalization of the magnetoelastic resonator in order to endow it with the proper selectivity toward the recognition of the desired analyte. A schematic representation of the described sensing process in that kind of sensors is shown in Figure 1.

Research on magnetoelastic materials is diversifying and enriching as the scientific community realizes the potential that this advanced technology holds for the design of advanced functional sensors. Magnetoelastic sensors have been already employed and specifically adapted to measure physical parameters such as viscosity,[16] density,[17] temperature,[18] or pressure,[19] and further functionalized with active layers to respond to pH,[20] humidity,[21] volatile organic compounds (VOCs),[22] or heavy metals,[23] or even to biological agents such virus or bacteria.[24,25]

Thus, the scope of this review is to bring the potentials of magnetoelastic sensors to all the related research areas by reviewing in an illustrative manner the most recent advances achieved to improve the overall response of magnetoelastic transducers, and the varied strategies that have been applied to functionalize their surface in order to endow them with specific sensing functionalities. To this end, we have first described the fundamentals of magnetoelasticity, a phenomenon on which magnetoelastic devices are based as well as the fundamentals and equations governing magnetoelastic sensor performance. Then, the specific strategies applied to tune and improve the functionality and applicability of the magnetoelastic based transduction for biological, chemical, and physical sensing have been identified. Finally, the most recent advances to further improve the overall response of magnetoelastic transducers have been outlined.

WORKING PRINCIPLE

AW devices are usually made of a material that presents a coupling effect between mechanical and optical, electrical, or magnetic energies. The detection process is based on the variation of those properties (optical, electrical, or magnetic) when exposed to different perturbations, which affects their mechanical properties such as mass loadings or viscosity changes. In the case of magnetoelastic sensors, they present a magnetoelastic coupling effect, i.e., an effective interchange of energy from magnetic to elastic (magnetostriction) and from elastic to magnetic (magnetoelasticity).[26] This effect is based on the dynamics of the magnetic domain, including their mobility or propagation in the magnetic substrate. At the atomic level, this coupling arises from the deformation of the crystal lattices inside the domains tending to align with the domain magnetization. When the atomic moments occupy their sites, they alter the bond lengths, deforming the crystal lattice. The magnetoelastic energy tends to align the bonds with the domain magnetization, but in counterpoise is the elastic bond energy. Macroscopically, the external applied magnetic field is adding energy to the system (ΔE_m) that is counterbalanced by the change in the elastic bond energy (ΔE_{el}) along the magnetic material:

$$\Delta E_m = \Delta E_{el} \Leftrightarrow \Delta M \cdot \Delta H = \frac{1}{2} k \Delta \lambda^2 \Leftrightarrow \frac{\Delta M}{\Delta H} = \frac{1}{2} k \left(\frac{\Delta \lambda}{\Delta H} \right)^2 \quad (1)$$

where k is the macroscopic elastic constant of the material and $\Delta\lambda$ is the elongation caused by the change in the ΔM magnetization.[27]

Thus, the cited magnetostriction effect (or Joule effect) consists of the relative deformation suffered by the ferromagnetic material when subjected to an external magnetic field (H).[26] Conversely, the magnetoelastic effect (or Villari effect) consists of the change in the magnetic state of the

https://doi.org/10.1021/acssensors.2c00032
ACS Sens. XXXX, XXX, XXX−XXX

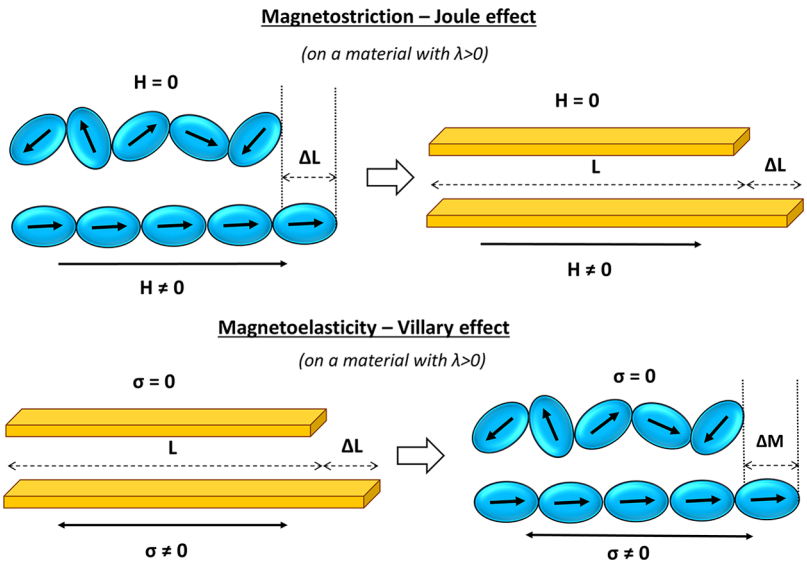

Figure 2. Scheme of the magnetostriction and magnetoelasticity effects on a magnetoelastic resonator with a positive magnetostriction coefficient ($\lambda > 0$).

material when a mechanical stress (σ) is applied. Both processes are schematically illustrated in Figure 2 for a material with a positive magnetostriction coefficient ($\lambda > 0$).

The dynamic behavior of these processes can result in elastic waves propagating along the magnetic substrate. This is the basis of the magnetostrictive delay line (MDL) technique, which has been extensively studied for sensing purposes.[27] Besides, when the frequency of the pulsed magnetic field applied to a freestanding magnetoelastic ribbon (with associated wavelength λ) matches with the length of the resonator L (in the following way: $L = n(\lambda/2)$, with n being an integer (n = 1, 2, 3, ...)), the magnetoelastic resonance frequency appears. The basis of the detection process of magnetoelastic AW devices is the dependence of that magnetic state of the material from external forces or mechanical loads. Thus, parameters such as temperature, viscosity, or mass loadings can directly affect the resonance frequency of the freestanding magnetoelastic ribbon, being detected as a shift of the frequency curve (Figure 1).

The theoretical value for this magnetoelastic resonance frequency has been modeled by different approaches and degrees of complexity.[28] In particular, the induced longitudinal vibration along the length direction (in the following, supposed to be the X-axis) of a magnetoelastic resonator can be described by the eq 2 of motion:

$$\frac{\partial^2 u_x}{\partial t^2} = \frac{E}{\rho(1-\upsilon^2)}\frac{\partial^2 u_x}{\partial x^2} \tag{2}$$

where E is Young's modulus, ρ is the density, and ν is the Poisson coefficient of the magnetoelastic material. The displacement function ($u(x, t)$) of the longitudinal elastic wave propagating along the length direction of a rectangular ME resonator of length L is given by

$$u(x, t) = u_o \cos\left(\frac{n\pi}{L}x\right) e^{i2\pi f_n t} = u(x)\, e^{i2\pi f_n t} \tag{3}$$

where u_0 is a constant and f_n is the resonance frequency of the nth harmonic mode. By solving the preceding equations, the theoretical equation for the resonance frequency of a freestanding rectangular-shaped magnetoelastic resonator of length L is obtained as

$$f_r = \frac{n}{2L}\cdot\sqrt{\frac{E}{\rho(1-\upsilon^2)}} \tag{4}$$

In conclusion, the magnetoelastic resonance frequency is directly proportional to the resonance mode (n) and inversely proportional to the resonator length (L).

The first five consecutive resonance modes of a magnetoelastic resonator follow a similar tendency to that represented in Figure 3a. Moreover, in close relation to the previous insights, the resonance frequency and quality of a magnetoelastic resonator also depend on its length and shape, which result in a quite useful tool to improve the response of these types of transducers. This concept is illustrated in Figure 3b, where the resonance curves for Metglas 2826MB rectangular magnetoelastic resonators of 20, 15, and 10 mm in length are represented.

As can be observed in both cases, the increase on the resonance frequency is accompanied by a reduction in the amplitude and quality of the signal. Nevertheless, as will be detailed later, the higher the resonance frequency, the better the sensitivity of the transducer to a perturbation. For that reason, finding the ideal sensor's working conditions (resonance mode and resonator size) is key to boosting its sensing performance. In particular, most of the studies on magnetoelastic sensors work in the first resonance mode to gain signal quality, but works focusing on higher resonance modes (n = 2, n = 3···) are becoming more and more frequent in order to find out the best performance in terms of sensitivity.[29,30]

Something similar happens when selecting the sensor size, and most investigations on magnetoelastic sensors look for a compromise between the reduction on the signal quality and the increase of the sensitivity. As an illustrative example, Table 1 summarizes the resonance frequency and mass sensitivity dependence on resonator size for different magnetoelastic materials and analytes. In line with the conclusions stated above, the reduction on the resonator size seems to be a key factor to increase the mass sensitivity (up to Hz/pg). In

https://doi.org/10.1021/acssensors.2c00032
ACS Sens. XXXX, XXX, XXX−XXX

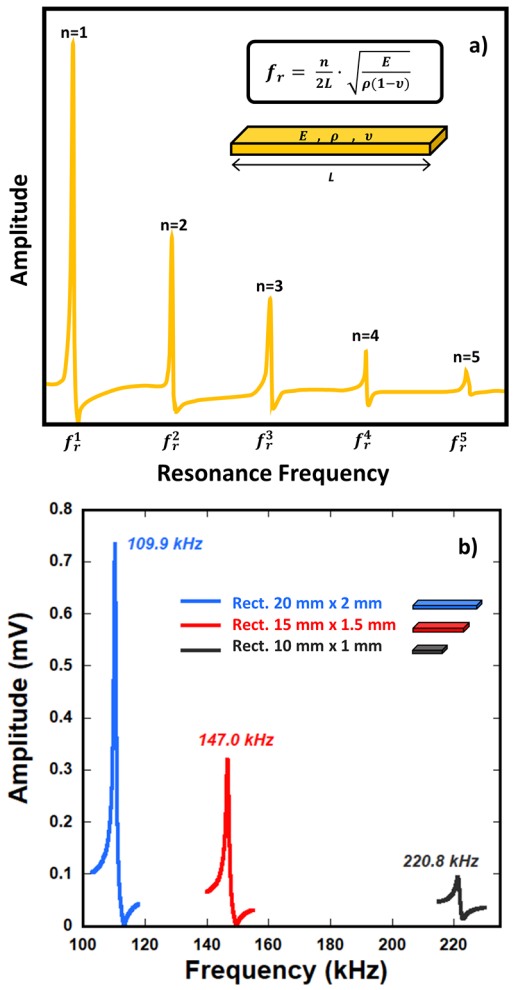

Figure 3. (a) First five resonance frequency modes measured for a rectangular magnetoelastic resonator of length L, Young's modulus E, density ρ, and Poisson ratio υ. (b) Magnetoelastic resonance frequency curves measured for rectangular Metglas 2826MB resonators o with different lengths.

Table 1. Resonance Parameters and Mass Sensitivities of Different ME Sensors with Different Compositions and Sizes Towards Different Analytes

ME material	Size	f_r (kHz)	S (Hz/μg)	ref
Metglas 2826MB	25 × 5 mm	87725	1.22	31,32
	25 × 2.5 mm	88175	2.22	
	20 × 2 mm	109.9	4.5	
	15 × 1.5 mm	147.0	12.6	
	10 × 1 mm	220.8	47.2	
$Fe_{64}Co_{17}Si_{6.6}B_{12.4}$	30 × 2 mm	67	7.5	33
	20 × 2 mm	102	18.1	
	10 × 2 mm	206	52.4	
		f_r (MHz)	S (Hz/pg)	
$Fe_{79}B_{21}$	1000 × 200 μm	2000	0.042	34
	500 × 100 μm	4000	0.338	
	250 × 50 μm	8000	13.5	
	100 × 20 μm	20000	333.3	

contrast, the decrease in size implies a reduction in the active area that can be functionalized to recognize certain substrates. A deeper insight on the modifications of the magnetoelastic parameters through its size and shape tuning will be given in the following sections.

Moreover, the magnetoelastic resonance frequency value, as well as its amplitude, also depend on the applied bias magnetic field. Figure 4a shows a representative curve of the dependence

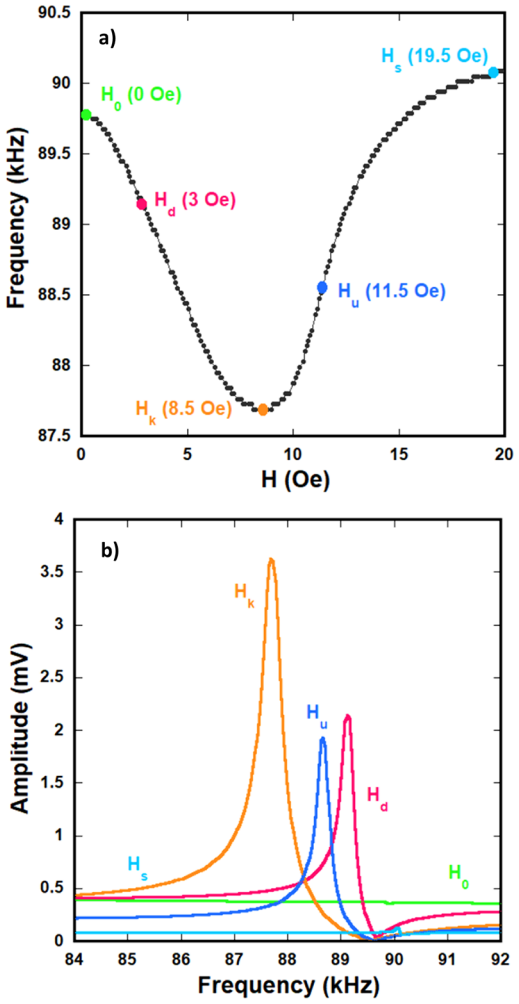

Figure 4. (a) Dependence of the magnetoelastic resonance frequency with the applied bias magnetic field in a rectangular Metglas 2826MB resonator (25 mm × 5 mm × 30 μm). (b) Resonance frequency curves measured at the different bias magnetic fields marked in the part a.

of the magnetoelastic resonance frequency with the DC magnetic field measured for a 25 mm × 5 mm rectangular magnetoelastic resonator. Five characteristic magnetic measuring fields have been highlighted in this curve with colored points, and the corresponding ME resonance curves measured in these fields have been plotted in Figure 4b. The fields represented in that curve are the minimum applied field (H_0), the applied field at which the resonance frequency is minimum, which is related to the anisotropy field (H_k), and the magnetic field at the magnetic saturation (H_s). The H_d and H_u fields are intermediate among the other fields, but interesting for the sake of comparison.

As can be observed, the bias magnetic field clearly affects the resonance frequency value as well as the signal intensity and quality. Actually, the main characteristic parameters of a magnetoelastic resonator can be derived from the magne-

https://doi.org/10.1021/acssensors.2c00032
ACS Sens. XXXX, XXX, XXX−XXX

toelastic resonance frequency curve as well as from its dependence on the applied magnetic field. In particular, the Young's modulus (E) (and the derived ΔE effect) and the magnetoelastic coupling coefficient (k) of a magnetoelastic resonator could be obtained from the resonance frequency curve by using eqs 5 and 6, respectively.[35,36]

$$E(H) = \rho(1 - \upsilon^2)(2Lf_r)^2 \tag{5}$$

$$k^2 = \frac{\pi^2}{8}\left[1 - \left(\frac{f_r}{f_a}\right)^2\right] \tag{6}$$

where E is the Young's modulus, ρ is the density, ν is the poisson coefficient, L is the length, and f_r and f_a are the resonance and anti-resonance frequencies, respectively. As can be observed, the Young's modulus, as the resonance frequency, highly depends on the applied magnetic field, with its minimum value located at the anisotropy field (H_k), and the maximum value at the magnetic saturation (H_s). That dependence of the Young's modulus with the applied magnetic field, known as the ΔE effect, is the most interesting and clear indicator of magnetoelasticity, and depends on factors such as the length to width ratio, the geometry, or the composition of the magnetoelastic ribbon. The ΔE factor can be derived from the maximum (E_s) and minimum (E_{min}) values of the Young's modulus[37] by using eq 7.

$$\Delta E(\%) = \frac{E_s - E_{min}}{E_s}\cdot 100 \tag{7}$$

With respect to the magnetoelastic coupling coefficient, its tendency versus the applied field is inverse to that of the Young's modulus, with the maximum magnetoelastic coupling coefficient located at the anisotropy field. For that reason, together with the higher signal amplitude at this characteristic magnetic field, sensing experiments are usually performed at the anisotropy magnetic field of the resonator.

Moreover, there is another critical parameter that defines the good performance of magnetoelastic resonators: the quality factor (Q). This parameter is associated with damping effects and quantifies the energy lost by the resonator. Therefore, the higher the Q value, the lower the energy losses and the narrower and sharper the resonance curves. Oppositely, a small Q value is related to a higher rate of energy losses and wider resonance curves. This factor can be directly obtained from the resonance frequency curve and is commonly calculated by using eq 8:

$$Q = \frac{f_r}{\Delta f} \tag{8}$$

where f_r is the resonance frequency and Δf is the full width at half-maximum intensity.[38] Recent works have reported new methods for a more accurate determination of this factor by numerical fitting of the magnetic susceptibility.[39]

All these parameters characterize the performance of magnetoelastic devices, but certainly, the operation of these devices as sensors is specially defined by its sensitivity, which is related to the resonance frequency shift observed under a specific perturbation on its surface (such as a mass load or a viscosity change). The changes suffered by a ME resonator under a mass loading or a viscosity change are described throughout the following sections.

Mass Loading Effect. The resonance frequency shift that a magnetoelastic resonator suffers under a mass loading is described as follows. When a mass loading (Δm) is uniformly deposited on the ME resonator surface, the density (ρ) value in eq 2 is replaced by ρ_{load}

$$\rho_{load} = \frac{m_0 + \Delta m}{A\cdot t} \tag{9}$$

where m_0 is the mass of the bare resonator, A its surface area, and t the thickness. Thus, solving eq 2 using the corresponding ρ_{load}, the resonance frequency of the loaded resonator is calculated to be

$$f_m = \frac{n}{2L}\sqrt{\frac{1}{1 + \Delta m/m_0}\frac{A\cdot t}{m_0}\frac{E_s}{(1-\sigma^2)}} = f_0\sqrt{\frac{1}{1 + \Delta m/m_0}} \tag{10}$$

and for small mass loads in comparison with the resonator mass, the resonant frequency shift of the system is approximated by eq 11[40]

$$\Delta f = f_m - f_0 = -f_0\frac{\Delta m}{2m_0} \tag{11}$$

Thus, the magnetoelastic resonator mass sensitivity (S) is calculated tobe

$$S = -\frac{\Delta f}{\Delta m} = \frac{f_0}{2m_0} \tag{12}$$

where Δf is the measured resonance frequency shift, Δm is the loading mass, and m_0 and f_0 are the mass and the resonance frequency of the bare magnetoelastic platform.[30] Hence, a higher resonance frequency or a lower resonator mass is translated into an overall higher sensitivity value. It should be noted that this relationship is just an approximation of a more general expression, and it is not always valid to explain the frequency shift. For this reason, expanded equations are sometimes applied to adjust more complex experimental data.[41]

It should be noted that the mass loading effect on the ME resonator is the basis of chemical or biologic agent sensing, in air or liquid media. To achieve a selective sensing of these targets, a specific surface functionalization of the metallic ribbons used as magnetoelastic resonators is required. The most frequently employed active layers curently will be reviewed two sections later.

Density and Viscosity Effects. When a magnetoelastic resonator is immersed in a liquid, the magnetoelastic resonance frequency and the signal amplitude vary as a function of the viscosity and density of the media due to the damping effects. That frequency shift (Δf) depends on both the density (ρ_l) and the viscosity (η) of the fluid that surrounds the resonator, and its value is commonly approximated by[16]

$$\Delta f = \frac{\sqrt{\pi f_0}}{2\pi\rho_s d}\sqrt{\eta\rho_l} \tag{13}$$

where d and ρ_s are the thickness and density of the resonator, respectively.

Thus, parameters such as mass and viscosity (among many others) could be easily measured by tracing the resonance frequency shift under a mass load or under a viscosity change,

https://doi.org/10.1021/acssensors.2c00032
ACS Sens. XXXX, XXX, XXX−XXX

respectively. In this regard, the most significative and recent advances and applications of mass and viscosity ME-based sensing devices are collected in the following sections, including surface functionalization processes and a series of strategies to increase their sensitivity. Previously, the type of magnetoelastic platforms usually employed for that must be detailed.

MAGNETOELASTIC RESONATORS—COMPOSITION AND FABRICATION

Magnetoelastic Alloy Composition. Magnetoelastic resonators consist of amorphous ferromagnetic alloys, usually obtained as iron-rich metallic glasses that are partially alloyed with nickel or cobalt, as well as doped with other metals in smaller proportions (such as boron, molybdenum, or silicon). The accessible compositional variance results in a large number of alloys with very different values of spontaneous magnetization, Curie temperature, magnetostriction constant, crystallization temperature, and corrosion resistance, among others.[42]

In particular, Metglas 2826MB iron-rich amorphous ferromagnetic alloy has been the most employed material as a magnetoelastic platform for sensing applications until the present date. Its high saturation magnetostriction (12 ppm) and saturation magnetization (0.88 T) are two of the reasons for its wide use as a transducer.[43,44] It is important to mention that in addition to being a low-cost material, Metglas 2826MB is already industrially produced and commercially applied. Besides, this alloy shows high corrosion resistance which makes it suitable to be used in harsh environments, opening the prospects for its application for biological or chemical sensing purposes. The most important chemical, physical, and magnetic properties of Metglas 2826MB are summarized in Table 2.[37,45,46]

Table 2. Magnetic, Physical, and Chemical Properties of Metglas 2826MB Alloy[37,45,46]

Magnetic and Physical Properties		Composition	
Saturation Magnetization (T)	0.88		
Magnetoelastic Coupling	0.30	Element	Weight (%)
Saturation Magnetostriction (ppm)	12	B	1-5
Curie Temperature (ºC)	353	Fe	40-50
Crystallization Temperature (ºC)	410	Mo	5-10
Density (g/cm³)	7.90	Ni	40-50
Elastic Modulus (GPa)	100-110	Co	<0.3

Although Metglas 2826MB is the most employed ME material for sensing applications, other alloys, both commercially available as well as home-fabricated, have been employed and improved during recent years. Examples of commercially available alloys, alternatives to Metglas 2826MB, employed for magnetoelastic sensing include other Metglas alloys[47] such as Metglas 2605SA1 ($Fe_{90}Si_5B_5$), Metglas 2826CO ($Fe_{67}Co_{18}B_{14}Si_1$), or Metglas 2605S3A ($Fe_{77}Cr_2Si_5B_{16}$); as well as Vitrovac type alloys,[28] such as Vitrovac 4040 ($Fe_{39}Ni_{39}Mo_4Si_6B_{12}$) or Vitrovac 7600 ($Fe_{64.5}Co_{18}B_{16}Si_1C_{0.5}$). In addition, intensive research is ongoing to develop homemade alloys with improved magnetoelastic properties, as in the cases of $Fe_{77.5}Si_{7.5}B_{15}$,[48] $Fe_{79}B_{21}$,[49] $Fe_{83}Ga_{17}$,[50] or $Fe_{64}Co_{17}Si_{6.6}B_{12.4}$,[33] among others. In addition to the composition, the fabrication method and the subsequent post-fabrication treatments (such as thermal annealing) significantly influence the properties of the metallic glass.

Magnetoelastic Alloy Fabrication, Shaping, and Post-Treatments. As mentioned before, fabrication technology of magnetoelastic resonators is in a mature stage, allowing the cheap and mass production of a varied scope of magnetoelastic alloys, as well as their easy shaping in different forms and compositional modification. Magnetoelastic ribbons are industrially fabricated by sputtering deposition,[49] thermal evaporation,[51] or melt spinning[52] techniques, with the last one being the most mature technology from an industrial production point of view. Images of magnetoelastic tapes fabricated by melt spinning and by sputtering are shown in Figure 5 together with the identification of the main advantages (green) and disadvantages (red) arising from both processes.

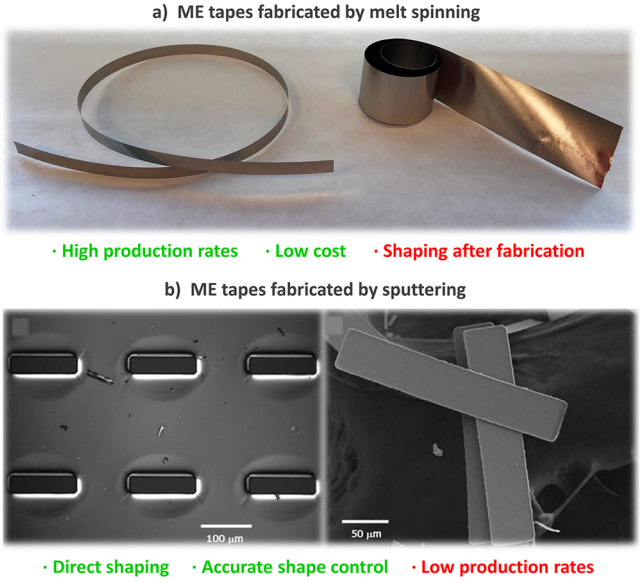

Figure 5. Images of ME tapes fabricated by (a) melt spinning and (b) sputtering techniques. Reproduced with permission from ref 49. Copyright (2009) Elsevier.

After the ribbon's fabrication, they are usually shaped into the final device with the proper size and geometry. A dicing saw,[53] scissors,[54] polishing and dicing,[55] computer numerical control (CNC) milling,[56] or picosecond pulsed laser ablation[28] are among the state-of-the-art techniques to achieve this end. In parallel, it is important to note that direct formation and shaping of the resonators by microelectronics fabrication (e.g., sputtering + lift-off) has been also reported.[57] The shaping technique for magnetoelastic resonators is of special concern, since it needs to be the most repetitive as possible while avoiding the generation of edge defects in the final resonator.

Moreover, ME resonators have been also subjected to postfabrication treatments in order to improve their signal quality or their corrosion resistant by changing the composition and size or by annealing the resonators while exposed to a transverse magnetic field. In particular, annealing treatments have been applied in order to increase the magnetoelastic coupling and the ΔE effect of the magnetoelastic alloy[58] while releasing the residual stress arising from its fabrication and shaping.[59] Moreover, the corrosion resistance of magnetoelastic resonators is another concerning

https://doi.org/10.1021/acssensors.2c00032
ACS Sens. XXXX, XXX, XXX−XXX

parameter, especially when working in aggressive environments. That is why different works have already investigated the degradation process of magnetoelastic sensors[60] and analyzed the effect of the resonator composition on their corrosion resistant.[61,62] In parallel, magnetoelastic alloys can be further coated with protective layers both to improve the sensor performance and to increase its chemical resistance. Chromium and gold metallic protective layers or polymer coatings are usually deposited on the resonator surfaces in order to improve the adhesion, biocompatibility, or anticorrosion properties.[55,63,64]

Deeper details of the current research in this direction will be given in the following sections, which are specifically focused on the application areas of magnetoelastic resonators as well as on the most recent advances on their property improvement.

APPLICATION FIELDS OF MAGNETOELASTIC RESONANCE DEVICES

Versatility of magnetoelastic resonators has paved the way to their application as wireless sensors of varied physical, chemical, and biological parameters. As stated before, it is important to note that a magnetic resonator can be directly applied without further modifications to measure physical properties as temperature, density, or viscosity.[17,18] In this specific case, the performance of the resonator in terms of its magnetoelastic properties will define the final assessment of the sensor. For chemical and biological sensing, the layer deposited onto the magnetoelastic resonator is the active part of the device that confers the capacity and selectivity to capture the target compound. In parallel, the magnetoelastic resonator transduces the mass adsorbed by the active layer (Δm) in a measurable magnetoelastic frequency shift (Δf). By varying the type of the active adsorbent layer (i.e., polymers, biomolecular recognition elements, metal oxides, nanoparticles, zeolites, or MOFs), different physical, chemical, and biological parameters such microorganisms, heavy metals, carbon dioxide, or VOCs have already been detected through magnetoelastic transduction. All the sensing applications based on magnetoelastic resonators explored up to date, together with a brief description of the magnetoelastic resonator, the active layers employed, and the main parameters describing their overall performance, are summarized in Tables 3−5.

Table 3. Different Physical Parameters Detected Using Magnetoelastic-Based Sensors

Analyte	Magnetoelastic material and size	Active layer	ref
Viscosity (glucose and polyethyleneimine)	Metglas 2826 (37.5 mm × 12.5 mm)	--	16
Density and viscosity simultaneously	Metglas 2826 (30 mm × 3 mm)	TiO_2 layer	17
VOCs and blood viscosity	Metglas 2826 (37 mm × 6 mm)	--	29
Blood plasma viscosity	Metglas 2826 (2 mm × 0.4 mm)	--	66
Ethanol	$Fe_{83}Ga_{17}$ wires (6−10 mm, Ø = 0.7 mm)	--	50
Air, water, and acetone viscosity	$Fe_{77.5}Si_{7.5}B_{15}$ wires (Ø = 125 μm)	--	48
Oil viscosity	Vitrovac 4040/Vitrovac 7600 (30 mm × 6 mm)	--	28

Application Fields of Bare Resonators: Viscosity and Density Sensors. Viscosity or density sensors based on magnetoelastic resonators generally do not need an active layer. In these cases, the resonance frequency shift is a consequence of the dissipative shear force created by the surrounding fluid, with the magnetoelastic shift dependent on the viscosity of the surrounding media.[65] By following this approach, Stoyanov and Grimes reported a sensor for monitoring the concentration of glucose dissolved in phosphate buffered saline (PBS) and also of polyethyleneimine dissolved in water.[16] The detection is based on the dependence of the resonant frequency with the square root of the viscosity and density product of the studied solutions (see eq 13). As the frequency shift is concurrently dependent on the liquid viscosity and density, it is not possible to differentiate both variables with a simple measurement. Therefore, Stoyanov and Grimes were only able to follow up the dependence of the resonance frequency shift with the square root of the viscosity and density product. Going a step beyond, Grimes et al. applied two magnetoelastic sensors for the simultaneous and individual determination of viscosity and density parameters.[17] For that, magnetoelastic resonators with the same size but different surface roughness (one with a TiO_2 coating layer and the other uncoated) were employed. Then, from the difference between frequency shifts measured for both samples, the density and viscosity of the liquid were successfully estimated. Along the same line, Cheng et al. reported a magnetoelastic sensor able to measure the viscosity of blood by comparing the sensitivity of five resonance modes under different liquid media (acetone, methanol, ethanol, etc.) with similar densities but varied viscosities.[29] Thus, after suppressing the density effect in the calibration curve, Cheng and co-workers were able to analyze and estimate the blood viscosity accurately. The key point of this research was the opposite responses of the first and fifth resonance modes to the density and viscosity of the media. While the first resonance mode exhibits better signal resolution, the highest mode was the most sensitive to viscosity changes (Figure 6). Finally, they validated the magnetoelastic sensor in human blood samples (i.e., blood from healthy person, anemic patient, and a patient with polycythemia vera) confirming that the resonance frequency was inversely proportional to the rate of red blood cells in the samples,

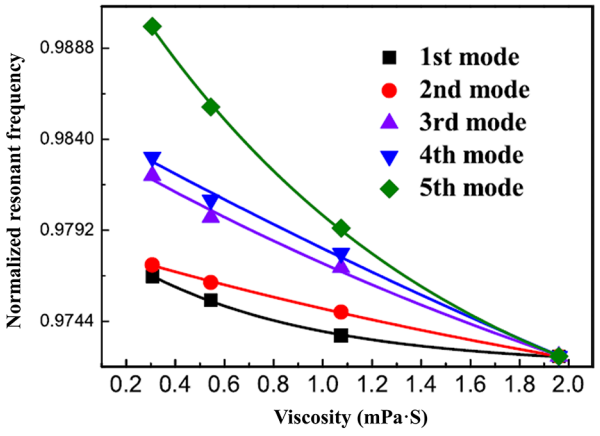

Figure 6. Normalized resonance frequency as a function of the viscosity for the first five resonance modes in a Metglas 2826MB resonator. Reproduced with permission from ref 29. Copyright (2015) IOP Publishing.

https://doi.org/10.1021/acssensors.2c00032
ACS Sens. XXXX, XXX, XXX−XXX

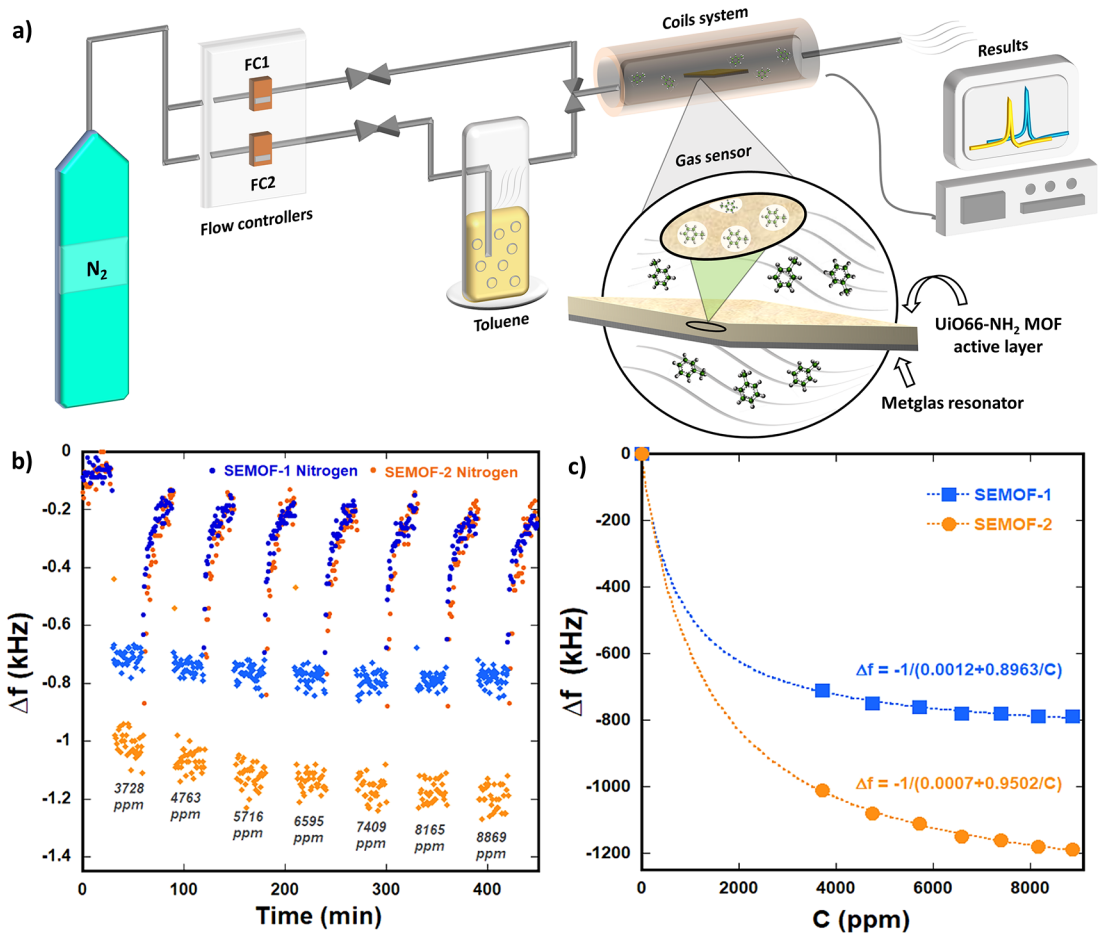

Figure 7. (a) Scheme of the experimental setup used for the toluene sensing experiments. (b) Toluene sensing experiments results for two different active layer mass. (c) Resonance frequency shift as a function of the toluene concentration. Reproduced with permission from ref 72. Copyright (2020) RSC Publishing.

which is directly related to the blood viscosity. A similar approach was followed later by Chen et al. by first calibrating the magnetoelastic resonator in glycerol/water mixtures of different densities and viscosities, and later on developing the in situ measurement of the blood plasma viscosity.[66] The frequency shift dependence on the plasma percentage in the mixture makes the magnetoelastic sensor capable of determining blood plasma viscosity values outside of the normal range.

The estimation of a lubricant viscosity is also of high importance to ensure the proper operation of many devices, including industrial machinery processes. In this regard, Bravo et al. applied Vitrovac magnetoelastic resonators for the sensing of lubricant oil viscosity.[28] By analyzing the damping of the magnetoelastic resonance (which depends on the viscosity of the surrounding medium) and modeling the experimental data by a least-squares fitting, they were able to determine the main parameters characterizing the magnetoelastic resonance as a function of the oil viscosity. These results open the perspective to a fast estimation of the oil viscosities, which are closely related to the quality and end of useful life of lubricants.

The main applications of ME resonators to detect physical parameters are summarized in Table 3.

Application Fields of Functionalized Resonators: Chemical and Biological Sensing. The functionalization of the resonator surface with active layers able to detect or interact with specific analytes opens the perspective to the application of magnetoelastic transducers for the detection of chemical and biological targets. The selection and integration of the active layer within the magnetoelastic resonator is key to achieving the best sensor in terms of selective, fast, and recoverable response. Indeed, it is important to reiterate that magnetoelastic resonators transduce mass loadings, so the higher the amount of analyte immobilized in the active layer, the higher the frequency shift induced. Therefore, the mass of the active layer as well as its capacity and specificity to capture the chemical or biological pathogen targets are parameters of paramount importance to amplify the magnetoelastic response of the resonator, and especially its mass sensitivity. Jointly, the characteristics of the active layer, of the resonator, and of their mutual integration will define the sensor'a final performance.

Sensing of Chemical Compounds and Chemical Reactions. Magnetoelastic resonators have also been employed for the detection of different chemicals in air or aqueous media. Regarding the monitoring of harmful gases, magnetoelastic transducers have been applied to sense greenhouse effect gases as carbon dioxide, corrosive gases as ammonia, or harmful volatile organic compounds (VOCs) as benzene, hexane, xylene, or toluene, among others. As mentioned before, the selection and integration of the active layer on the resonator surface play a key role in the selectivity toward specific compounds.

The first attempt in this direction was the work reported by Cai et al. for the detection of CO_2 by using a poly(acrylamide-*co*-isooctyl acrylate) copolymer functionalized resonator.[67]

https://doi.org/10.1021/acssensors.2c00032
ACS Sens. XXXX, XXX, XXX−XXX

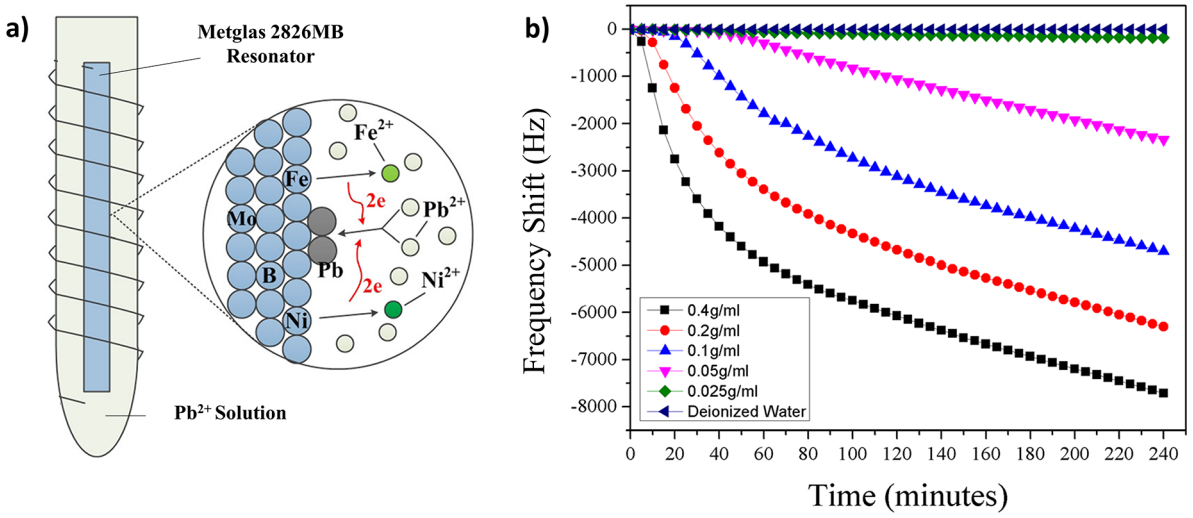

Figure 8. (a) Scheme of the reaction mechanism between the Pb^{2+} in solution and the Fe and Ni elements on the Metglas resonator. (b) Resonance frequency shift as a function of time for the ME resonator immersed in $Pb(NO_3)_2$ solutions with different concentrations. Reproduced with permission from ref 76. Copyright (2016) AIP Publishing.

They analyzed the effect of the copolymer active layer mass on the CO_2 sensing response of the resonator platform. They achieved a response of 4.4 Hz/%.CO_2, estimating a detection limit of 0.7% of CO_2 for a polymer with a 1:1 molar ratio of acrylic acid to isooctyl acrylate. Along the same line, Cai et al. developed a magnetoelastic sensor based on a poly(acrylic acid-*co*-isooctyl acrylate) copolymer as active layer for the detection of ammonia down to a 0.02% concentration.[68] Polymeric active layer-based resonators have also been applied to sense several VOCs. In particular, a magnetoelastic sensor functionalized with a Bayhydrol-110 polymer as the recognition layer was tested over eight different VOCs at different concentrations.[22] The results point out that the Bayhydrol-110/resonator sensor exhibits a very low response to hexane, but a high sensitivity to xylene (at least 10 times higher than for the other VOCs). Finally, the sensitivity of the sensor was further improved by increasing the mass of the active layer and decreasing the resonator length.

Besides polymers, inorganic-based functionalization of the resonators has been also applied to endow them with specific detection capabilities. Along this line, Zhang et al. applied Pt-TiO_2 coatings on magnetoelastic resonators for the detection of ethylene levels below 1 ppm.[69] They concluded that the thicker the active layer, the higher the frequency shift, but also the longer the time response due to lower diffusion rates of the analyte into the substrate. Later, Giannakopoulos et al. were the first to benefit from the porous and selective nature of zeolites (i.e., Faujasite) to assemble a magnetoelastic CO_2 sensor with an improved low detection limit of 0.33%.[70] Expanding the scope of this strategy, Baimpos et al. analyzed the effect of the zeolite type on the response of a magnetoelastic sensor to different VOCs.[71] FAU, LTA, MFI, and b-oriented MFI-type zeolites were directly grown on the surface of a magnetoelastic resonator, and the sensor response was tested over six different VOCs (such benzene, hexane, or xylene). The characteristics of the zeolite porosity was shown to shape the sensitivity and selectivity of the system to detect specific VOCs. For instance, a randomly oriented MFI active layer presents the highest sensitivity to *n*-hexane, the FAU exhibits the minimum detection limit for *o*-xylene, and the LTA-based sensor shows the highest selectivity to xylene isomers.

More recently, metal−organic framework (MOF) porous materials have also been employed as active layers for VOC detection in magnetoelastic resonators with different shapes.[72,73] In particular, UiO66-NH_2 was employed as active layer on a rhombic magnetoelastic resonator.[72] The MOF-based sensor was tested for toluene detection, and the effect of the active layer mass on its performance was deeply analyzed by the authors. It was concluded that the larger the active layer mass, the higher the resonance frequency shift and the saturation capacity. Sensitivities up to 0.27 Hz/ppm were achieved with this novel sensor. Finally, the sensor's selective response was also investigated by measuring the frequency change under ethanol, water, and acetone vapor atmospheres, confirming that the highest frequency change was measured under the presence of toluene. A scheme of this last application together with the main obtained response curves are shown in Figure 7.

Magnetoelastic resonators have been further employed for detection purposes in liquid media, especially to quantify the water content on heavy metals (HMs). In particular, Zhao et al. developed magnetoelastic-based sensors for the detection of uranium by two different methodologies based on the inhibition effect caused by the Uuranium in (i) the catalytic effect of Hg(II) on the precipitation reaction of potassium ferrocyanide with potassium ferricyanide[74] and (ii) the catalytic hydrolyzation caused by the α-amylase on a starch film deposited on the sensor surface.[75] In both cases, the increase in the uranium concentration reduces the catalytic effect leading to (i) a reduction on the sediment produced or (ii) a reduction in the starch film mass loss. The detection limit was increased from 0.46 μg/L, when employed the precipitation method, to 3.6 μg/L, when employed the α-amylase catalytic hydrolyzation. Similarly, Huang et al. reported a Hg(II) sensor based in the formation of thymine (T)-Hg structures in the presence of Hg(II) in aqueous solutions, which led to the release of complementary DNA (CDNA).[23] To this end, the magnetoelastic platform was functionalized with a graphene oxide active layer, which adsorbs the released CDNA, and hence leads to a resonance

https://doi.org/10.1021/acssensors.2c00032
ACS Sens. XXXX, XXX, XXX−XXX

Table 4. Different Chemical Parameters Detected Using Magnetoelastic-Based Sensors

Analyte	Magnetoelastic material and size	Active layer	Detection limit/sensitivity (S)	ref
CO_2	Metglas 2826 (38 mm × 9 mm)	poly(acrylamide-*co*-isooctyl acrylate) copolymer	0.7% CO_2; S = 4.4 Hz/% CO_2	67
Ammonia	Metglas 2826 (39 mm × 12.7 mm)	(poly(acrylic acid-*co*-isooctylacrilate) copolymer	0.02% NH_3	68
Ethylene	Metglas 2826 (40 mm × 5 mm)	Pt-TiO_2 films	Less than 1 ppm	69
CO_2	Metglas 2826 (20 mm × 6 mm)	Zeolite (FAU)	0.33% CO_2	70
VOCs (×9)	Metglas 2826 (20 mm × 6 mm)	(BAYHYDROL- 110) polymer	S = 0.24 Hz/ppm	22
VOCs (×6)	Metglas 2826 (20 mm × 6 mm)	Zeolites (FAU, LTA and MFI.)	Up to 6 ppm	71
Toluene	Metglas 2826 (10 mm × 2 mm rhomb)	MOF (UiO66-NH_2)	S = 0.27 Hz/ppm	72
Uranium (U)	Metglas 2826 (18 mm × 6 mm)	Polyurethane protection film	0.46 μg/L	74
Uranium (U)	Metglas 2826 (10 mm × 3 mm)	PVA + starch gel	3.6 μg/L	75
Lead (Pb)	Metglas 2826 (37 mm × 6 mm − 3 mm × 6 mm)	--	S = 24 Hz/mg mL^{-1}	76
Mercury (Hg)	Metglas 2826 (18 mm × 6 mm)	Graphene oxide	0.885 nM	23
Pb^2	Metglas 2826 (5 mm × 1 mm)	Bovine serum albumin (BSA)	3.3 × 10^{-7} mol/L	11
Cd^2			2.4 × 10^{-7} mol/L	
Cu^{2+}			2.3 × 10^{-7} mol/L	
Calcium oxalate and brushite precipitation	Metglas 2826 (17 mm × 6 mm)	Acrylic resin to prevent from corrosion	S = 1.38 kHz/mg	63
Calcium oxalate precipitation	$Fe_{73}Cr_5Si_{10}B_{12}$ (20 mm × 2 mm)	--	--	77
Fe_3O_4 nanoparticles deposition	Metglas 2605S3A (40 mm × 5 mm)	--	1.1 × 10^9 NPs	47
CoNiFe nanowires deposition	Metglas 2826 (6 mm × 1 mm)	--	200 ng	53
Polymer deposition	$Fe_{64}Co_{17}Si_{6.6}B_{12.4}$ (10, 20, and 30 mm)	--	S = 52.4 Hz/μg	33
Polyethylene glycol degradation	Metglas 2826 (12.7 mm × 5 mm)	Polyethylene glycol	--	78

frequency shift. The sensor presents a linear response in the 2.8−88.9 nM range.

Along this line, Guo et at. reported the detection of multiple heavy metals (Pb^{2+}, Cd^{2+}, and Cu^{2+}) based on the precipitation of bovine serum albumin protein produced when that protein is in contact with the heavy metal ions.[11] It was found that the sensor was more sensitive to heavy metals with larger molecular weight.

Moreover, Sang et al. confirmed the capacity to sense lead with bare magnetoelastic resonators.[76] It was found that the replacement of the Ni and the Fe in the Metglas 2826MB resonator surface by the Pb^{2+} ions present in the solution led to an increase in the sensor mass, and hence to a decrease in the resonant frequency. Additionally, they performed a study of the resonator length effect on the sensitivity, confirming that shorter resonators lead to higher sensitivities. A scheme of the process and the results for the sensing response are shown in Figure 8.

Finally, bare magnetoelastic-based sensors have also been employed to follow up crystallization, precipitations, or the functionalization or degradation process of the resonator itself.

In that context, Bouropoulos et al. monitored the in situ formation and precipitation of calcium oxalate and brushite mineral salts.[63] In a similar way, Sisniega et al. reported recently the application of a $Fe_{73}Cr_5Si_{10}B_{12}$ amorphous ferromagnetic alloy to monitor the calcium oxalate precipitation, showing different frequency shifts depending on the reaction time and the concentration of the solutions.[77] The outstanding sensitivity of 1.38 kHz/mg reported for a 17-mm-length rectangular Metglas sensor allows real-time monitoring of the nucleation and crystal growth processes via magnetoelastic resonators.

Following this line, Atalay et al. reported the application of magnetoelastic sensors for the detection of Fe_3O_4 nanoparticle (NPs) and $Co_{12}Ni_{64}Fe_{24}$ nanowire (NWs) deposition on the resonator surface.[47,53] In these works, a dependence of the frequency shift on the NPs/NWs mass deposited was observed, with the minimum detectable number of NPs being about 1.1 × 10^9, while the minimum detectable weight of NWs was around 200 ng. In a similar way, Sagasti et al. reported the application of $Fe_{64}Co_{17}Si_{6.6}B_{12.4}$ resonators of different lengths to monitor the deposition of polystyrene (PS) polymer onto the magnetoelastic ribbons.[33] Consecutive polymer depositions were performed by dip coating, and resonance frequency shift was measured after each cycle.

Inversely, magnetoelastic sensors have also been employed to follow up the degradation process of the active layer incorporated onto their surface. For example, Zhang et al. analyzed the degradation behavior of a poly(ethylene glycol) layer by measuring the resonance frequency amplitude decrease as a function of time.[78] They demonstrated that magnetoelastic sensors provide a nondestructive method to monitor in situ the mass loss of the active layer. All these results demonstrated the versatility of ME based sensors for chemical detection. Those previously described are summarized in Table 4.

Sensing of Biological Compounds. Some of the most important applications in which magnetoelastic sensors have been employed are in the biological field. Since the assessment of their first bioapplication around the 2000s, magnetoelastic transducers have already been used in the detection of different biological parameters such virus, bacteria, or mutated DNA, or even in the tracking of cell growth or for the monitoring of force conditions on artificial bones.[8,79]

A special focus of interest for the research community is the detection of pathogens as bacteria and viruses. To this end, the surface of the magnetoelastic resonators is usually coated with antibody or phage biorecognition elements, allowing the resonator to capture/interact the target microorganism. Once captured, the mass gain induces the corresponding decrease on the resonance frequency that enables the analyte quantification. In particular, Ruan et al. were the first to describe the

https://doi.org/10.1021/acssensors.2c00032
ACS Sens. XXXX, XXX, XXX−XXX

Table 5. Different Biological Parameters Detected Using Magnetoelastic-Based Sensors

Analyte	Magnetoelastic material and size	Active layer	Detection limit/sensitivity (S)	ref
Staphylococcal enterotoxin B	Metglas 2826 (6 mm × 2 mm)	Antistaphylococcal enterotoxin B IgG	0.5 ng/mL	82
Bacillus anthracis spores	FeB alloy (500 μm × 100 μm)	Landscape phage	S = 1.2 kHz/ng	57
Bacillus anthracis spores	Metglas 2826 (2 mm × 0.4 mm)	Phage clone E2	10^5 spores/mL	96
Salmonella typhimurium and *Bacillus anthracis*	Metglas 2826 (2 mm and 1.9 mm)	E2 and JRB7 phages	5 × 10^3 CFU/mL	82
Salmonella typhimurium	Metglas 2826 (25 mm × 5 mm − 2 mm x 0.4 mm)	Rabbit polyclonal antibody	5 × 10^3 CFU/mL	83
Salmonella typhimurium (in milk)	Metglas 2826 (2 mm × 0.4 mm)	Phage clone E2	S = 118 Hz/decade	84
Salmonella typhimurium (on tomatoes)	Metglas 2826 (1 mm × 0.2 mm)	E2 phage	5 × 10^2 CFU/mL	85
Salmonella typhimurium (on eggshells)	Metglas 2826 (1 mm × 0.2 mm)	E2 phage	1.6 × 10^2 CFU/cm^2	86
Salmonella typhimurium (on spinach)	Metglas 2826 (1 mm × 0.2 mm)	E2 phage	--	87
Salmonella typhimurium	Metglas 2826 (1 mm × 0.3 mm)	E2 phage	Less than 100 cfu/mL	81
Listeria		Anti-*Listeria monocytogenes* rabbit IgG		
S. aureus		Anti-S. aureus IgG		
E. coli		Anti-*E. coli* rabbit IgG		
E. coli	Metglas 2826 (6 mm × 1 mm)	Anti-*E. coli* O157:H7 antibodies	10^2 CFU/mL	80
E. coli (in juices)	Vitrovac 7600 (1 mm × 0.2 mm)	Anti-*E. coli* polyclonal antibodies (pAb)	10^2 CFU/mL in water and 10^4 CFU/mL in juice	97
E. coli	Metglas 2826 (5 mm × 1 mm)	Anti-*E. coli* ab137967 and ab25823 antibodies	376 Hz/μg	98
E. coli and *S. aureus* (in milk)	Metglas 2826 (5 mm × 1 mm)	Silicon alkoxide precursors (TEOS and MAP)	--	25
Classical swine fever virus	Metglas 2826 (37 mm × 6 mm)	E2 glycoprotein and anti-CSFV E2 antibody	2.466 ng/mL S = 56.2 Hz/μg·mL^{-1}	24
Atrazine	Metglas 2826 (5 mm × 1 mm)	Atrazine antibody	1 ng/mL S = 3.43 Hz/μg mL^{-1}	99
Carcinoembryonic antigen	Metglas 2826 (5 mm × 1 mm)	DNA-AgNCs and DNA-AgNCs	1 pg/mL S = 105.05 Hz/ng·mL^{-1}	92
Mutated DNA	Metglas 2826 (5 mm × 1 mm)	Thiolated DNA	0.571 pM S = 72.7 Hz/nM	88
VKORC1 genes	Metglas 2826 (5 mm × 1 mm)	Different buffer solutions + biotin−DNA	0.00389 fM S = 45.7 Hz·pM^{-1}	89
Human serum albumin	Metglas 2826 (5 mm × 1 mm)	Anti-HSA IgG	0.01 μg/mL S = 9.3 Hz/μg·mL^{-1}	91
Glucose (in urine)	Metglas 2826 (18 mm × 6 mm)	pH-sensitive polymer + GOx and catalase	S = 61.9 Hz/mM	64
Hemoglobin oxidation	Metglas 2826 (2 cm length)	ZnO nanoparticles film	--	93
Cell growth	Metglas 2826 (12.7 mm × 5 mm)	Parylene-C	--	94
Gold degradation in cell culture	Metglas 2826 (5 mm × 1 mm)	Gold	--	95

application of magnetoelastic resonators for bacteria detection.[80] They employed Metglas resonators for *Escherichia coli* (*E. coli*) quantification by using an anti-*E. coli* antibody as the active layer attached to the resonator's surface. The results confirmed the feasibility of magnetoelastic platforms to detect bacteria down to a detection limit of 10^2 CFU/mL and with a linear response in a wide concentration range. This work paved the way for all the later studies that have been done in this area, as summarized in Table 5 and briefly described in the following section.

Since the pioneering work of Ruan et al., magnetoelastic biosensors have been employed to detect a varied scope of bacteria and viruses such as *Bacillus anthracis* spores, *Salmonella typhimurium*, *Listeria*, or *Staphylococcus aureus* (*S. aureus*), among many others.[81] Applicability of magnetoelastic biosensors goes beyond proof of concept ideal conditions. For example, Xue et al. confirmed the sensing response of Vitrovac resonators toward *E. coli*, achieving detection limits and linear response over a range of *E. coli* concentrations similar to that of the Metglas-based sensors.[82] Moreover, efforts in this area have been directed to detect pathogens not only in solutions but also in food, as in the example of *Salmonella typhimurium*, which is a health concern due to its well-known potential hazards. In particular, Guntupalli et al. were the first to investigate magnetoelastic sensors for *Salmonella* detection.[83] This work was performed in a solution containing the target bacteria in different concentrations. A detection limit of 5 × 10^3 CFU/mL was achieved using 2 mm × 0.4 mm Metglas functionalized resonators with polyclonal antibodies. Later, they expanded the possibility to sense *Salmonella* in different matrixes, such as milk,[84] tomatoes,[85] eggshells,[86] or spinach,[87] demonstrating good sensing capabilities and detection limits in the range of 5 × 10^2 to 5 × 10^3 CFU/mL. Along this line, a recent work by Beltrami et al. investigated the sensing of *E. coli* and *S. aureus* in milk by using a hybrid film based on silicon alkoxide precursors (TEOS and MAP) as the active layer, thus avoiding the use of antibodies.[25] This active layer allows one to detect the presence of bacteria in the media and, at the same time, protect the magnetoelastic resonator from corrosion.

To go a step forward, multiresonance platforms have given access to multiparameter biological sensing as well. This is the case of the work reported by Huang et al., which demonstrates the concurrent response of a multiple resonator for the detection of *Salmonella typhimurium* and *Bacillus anthracis* spores present in liquid media simultaneously.[10] Moreover, it is also observed that under exposure to a single pathogen

https://doi.org/10.1021/acssensors.2c00032
ACS Sens. XXXX, XXX, XXX−XXX

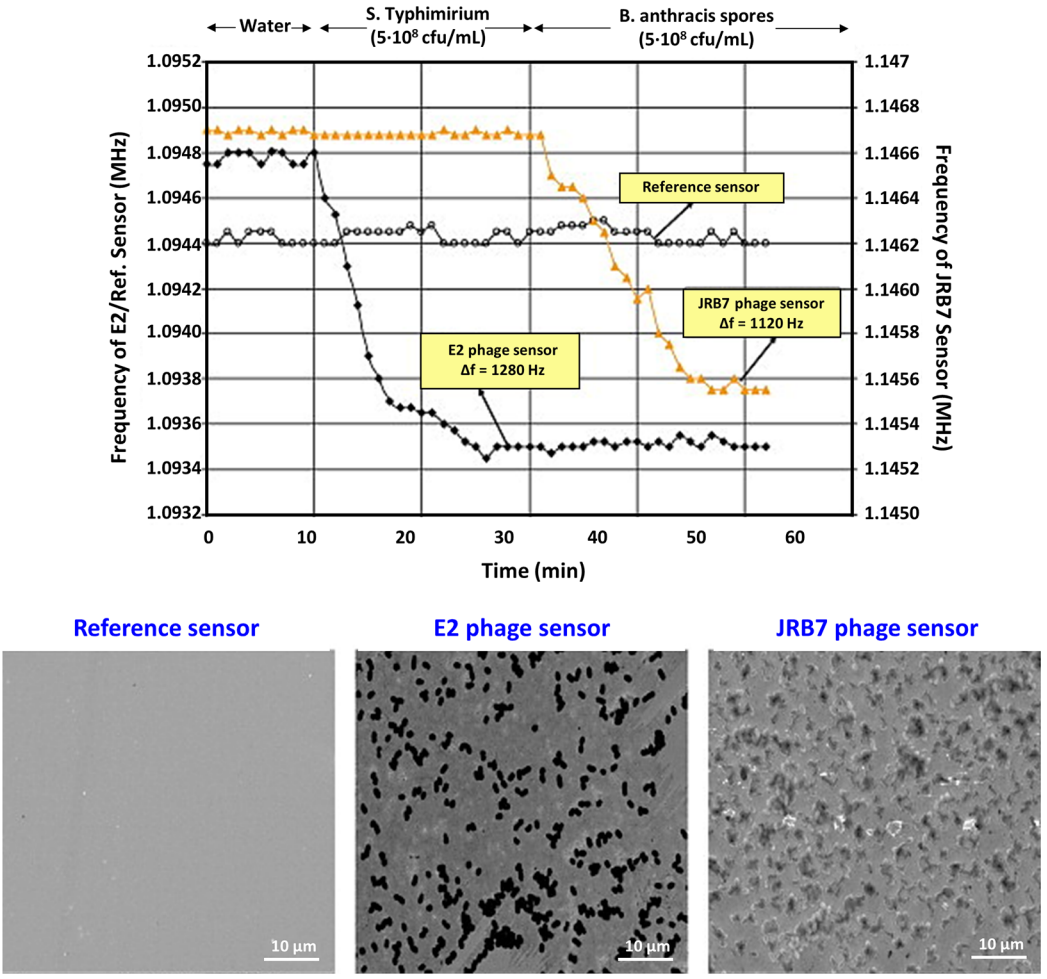

Figure 9. Response curves and surface SEM images for three different ME biosensors (reference sensor, E2 phage sensor, and JRB7 sensor) tested simultaneously under exposure to different pathogen solutions. Reproduced with permission from ref 10. Copyright (2009) Elsevier.

solution, only the resonator coated with the corresponding specific phage presents a response, which demonstrates the selective sensing capacity of these kind of multisensors. Figure 9 shows the response of these devices under exposure to different pathogen solutions.

Along this line, magnetoelastic sensors have given access to measurement of other biological parameters such mutated DNA, lysozymes, carcinoembryonic antigen (CEA), or human serum albumin (HSA), among others. In particular, Guo et al. investigated the detection of mutated DNA responsible for the β-thalassaemia blood disorder.[88] After complete functionalization of the ME resonator, it was tested for the mutated DNA (tDNA). The results indicate excellent selectivity and stability as well as a linear response with the concentration of this tDNA in the range of 1.0×10^{-8} M to 1.0×10^{-12} M, indicating the possibility of employing ME sensors for the cheap and wireless diagnosis of β-thalassaemia disease. In a similar way, Sang et al. expanded the use of ME sensors to detect warfarin doses by monitoring VKORC1 genotypes.[89] The biocompatibility of the ME sensor was improved using gold layers, while the functionalization with thiolated capture probes, tDNA, and biotin layers leads to a high sensitivity and specific detection. The fabricated sensors show fast and linear responses in the range of 0.1 fM to 10 pM, which demonstrates the possibility of employing cheap magnetoelastic sensors for the biomedical detection of warfarin doses, among others.

Recently, Huang et al. studied the application of Metglas resonators functionalized with a lysozyme antibody.[90] The biotarget-encoded sensor exhibits a high sensitivity (138 Hz/ μg·mL^{-1}) and a very low detection limit (1.26 ng/mL). In a similar way, Liu et al. expanded the potential uses of ME resonators to detect HAS.[91] For that, the Metglas ME resonators were first coated with chromium and gold layers to protect the sensor from corrosion, enhance the biocompatibility and sensitivity, and improve the immobilization of the antibodies. After that, anti-HSA IgG was immobilized on the gold functionalized ME resonator. The response of the immunosensor was linear, highly sensitive, fast, and reversible for HSA concentrations in the range from 0.01 to 100 μg/mL^{-1}. The outstanding specificity of this sensor for HSA detection was also demonstrated, in which the frequency shift caused by HAS is almost four times that caused by other biomolecules. Finally, Wang et al. applied ME sensors for CEA detection.[92] The sensor functionalization was similar to that previously described for HAS, but employing a CEA aptamer (Figure 10a). The immunosensor exhibits a varied response versus the CEA concentrations ranging from 0.002 to 6.25 ng·ml^{-1}, with stabilization times up to 40 min (Figure 10b). The high specificity toward CEA was one of the most remarkable characteristics of this sensor (Figure 10c).

Other biological parameters such as glucose concentration, hemoglobin oxidation, or cell growth tracing have been also

https://doi.org/10.1021/acssensors.2c00032
ACS Sens. XXXX, XXX, XXX−XXX

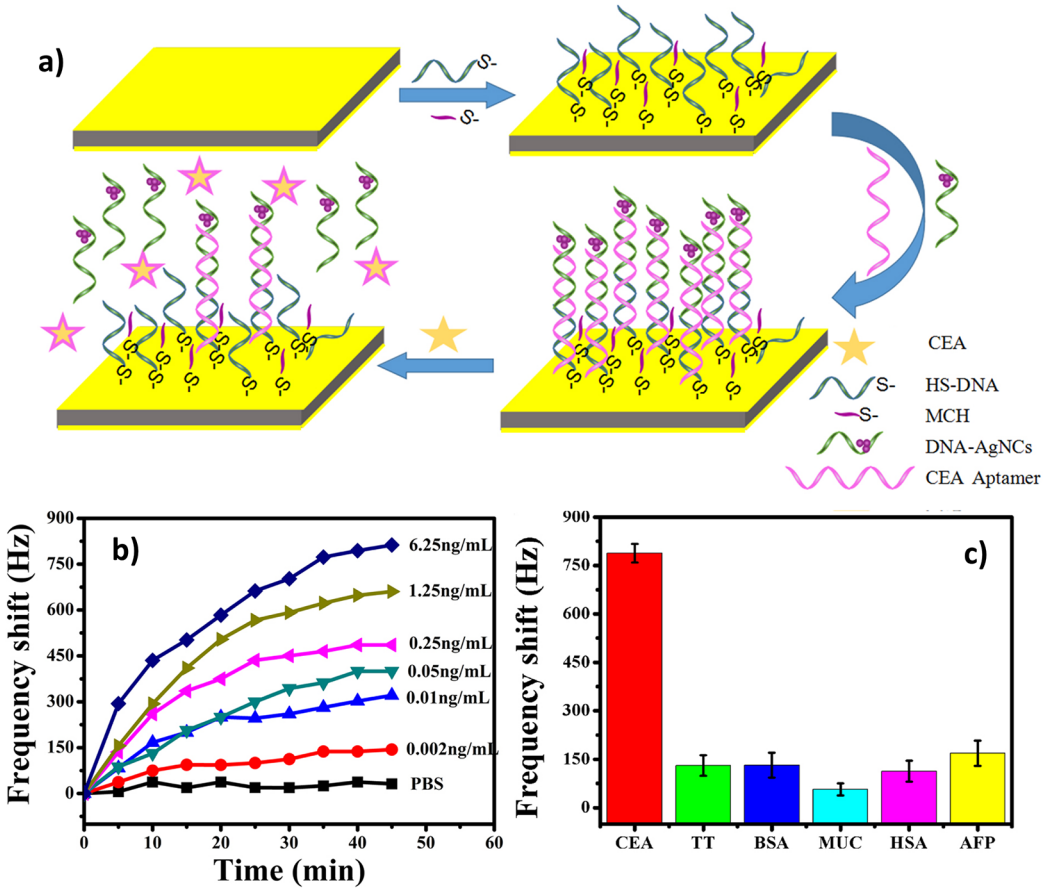

Figure 10. (a) Schematic diagram of the surface functionalization and detection procedure for the CEA immunosensor. (b) Real-time frequency response curves for CEA detection at different concentrations. (c) Specificity measurement for the CEA immunosensor. Reproduced with permission from ref 92. Copyright (2019) IOP Science.

detected based on other mechanisms. In particular, Gao et al. employed magnetoelastic resonators for the detection of glucose concentration in urine samples based on the glucose oxidase-catalyzed hydrolyzation of the glucose.[64] The frequency shift shows a linear response proportional to the glucose concentration between 1 and 15 mM. Based also on the detection of mass gains arising from chemical reactions, Sagasti et al. employed magnetoelastic resonators to detect hemoglobin oxidation.[93] Hemoglobin was immobilized on a zeolite active film and later oxidized by H_2O_2 addition. The system exhibited a linear response of the magnetoelastic resonance frequency versus the H_2O_2 concentration. Most recently, Shekhar et al. were able to follow up in real-time mammalian cell growth by using magnetoelastic resonators.[94] In this study, the magnetoelastic sensors were exposed to cell media with different seeding densities, in order to control the number of cells attached to the sensors and, in turn, to introduce a linear variation of the frequency shift of the system as a function of the cell numbers grown on the sensor.

Inversely, magnetoelastic sensors have been also employed to follow biological degradation processes. In particular, Menti et al. analyzed the degradation of a bare Metglas 2826MB resonator when exposed to cell culture and compared it with a gold-covered Metglas resonator.[95] By this analysis, they observed that the bare Metglas ribbons degrade on contact with the cell culture solution, causing a frequency shift and hence contributing to erroneous sensing results. On the contrary, the coating of the resonator with a gold layer protects the sensor from degradation and increases its biocompatibility.

Other relevant fields related to biosensing where magnetoelastic resonators have been successfully applied is the tracking of degradation rates and force conditions on bones.[100] In this case, the sensing principle is based on the mechanical stress produced in the magnetoelastic ribbons during bone degradation. Those applications have been already reviewed recently by Ren et al.,[43] and they will not be focus of deeper description in this work.

For most of the previously reviewed biological applications, the target phage/antibody is essential to achieve selective sensing.[101] Nevertheless, it should be noted that as important as the phage/antibody layers are, the ones that prevent the corrosion and improve the adhesion of the analytes are the magnetoelastic ribbons. The gold layers are the archetypal magnetoelastic resonator surface functionalization when applying them for biological sensing. In addition to antibody functionalization, the surface roughness also has an important effect to fasten bacteria detection or to induce a larger frequency shift when a thinned and polished surface is obtained.[98]

NOVEL STRATEGIES TO IMPROVE THE RESPONSE OF MAGNETOELASTIC SENSORS

As previously anticipated, there are three critical parameters that define the good performance of magnetoelastic resonators when working as mass detectors: (i) the sensitivity and the

https://doi.org/10.1021/acssensors.2c00032
ACS Sens. XXXX, XXX, XXX−XXX

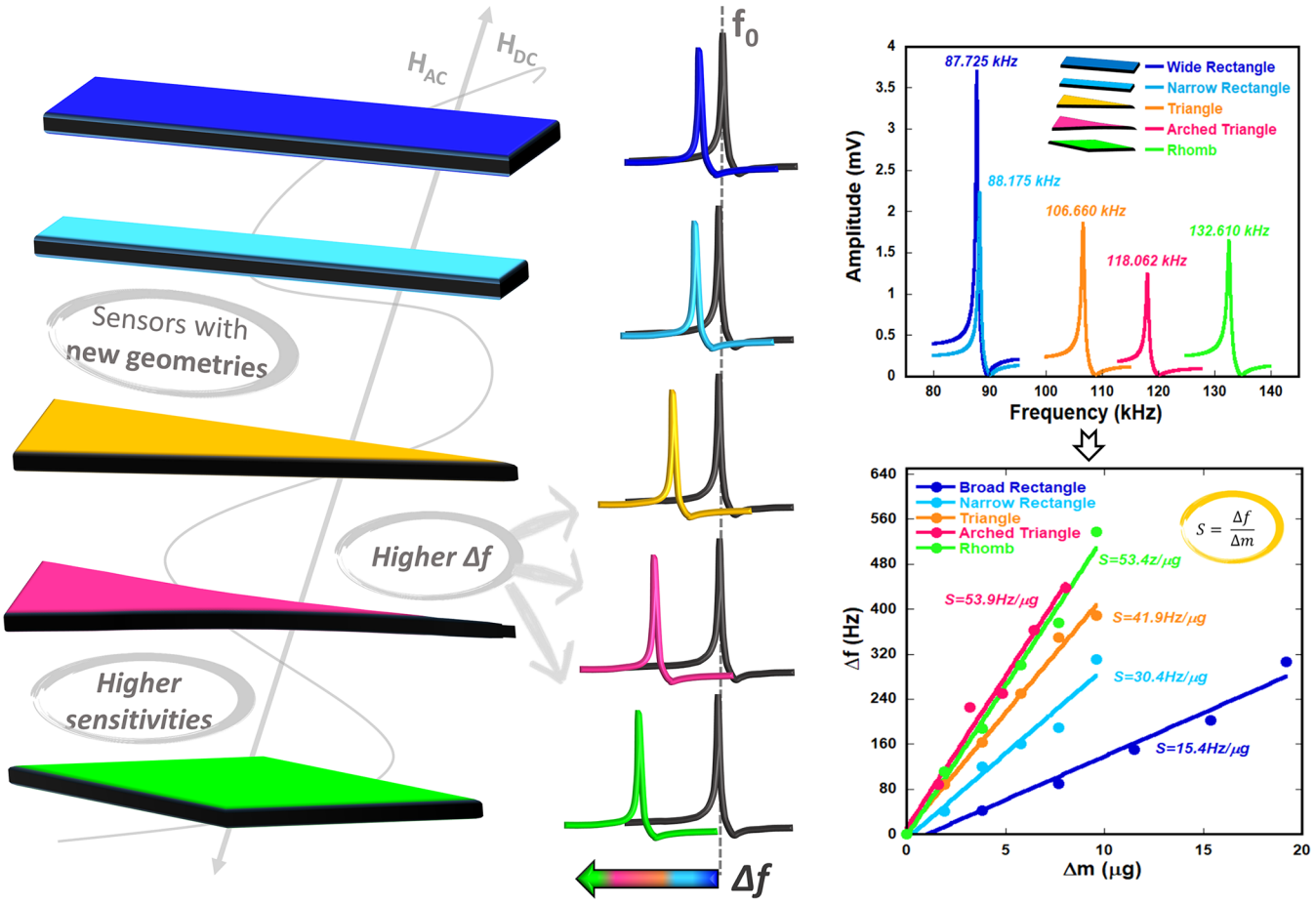

Figure 11. Scheme of the different geometries previously described and resonance frequency curves and mass sensitivities measured for each of these resonator geometries with a length of 12 mm.[31,32]

minimum detection limit, (ii) the resonance quality factor, and (iii) the corrosion resistance of the resonator. In this section, the most recent advances to improve the sensitivity of these devices are described.

Novel Geometries: Toward Highly Sensitive ME Resonance Sensors. Sensitivity is critical to assess the performance of any sensing device. In this context, the reduction of the transducer size is probably the most used technique to increase the mass sensitivity of the system.[33,102] This results from the increase of frequency associated with a reduction of the length of the ME resonator (eq 12).[33,102] The process of miniaturization requires the use of complex techniques such as sputtering (Figure 5b), and until recently, it was done while maintaining their classic rectangular geometry. However, the miniaturization of resonators also results in some drawbacks: the reduction of the resonance quality factor and the signal intensity. Moreover, edge defects, the lack of dimensional repeatability, and handling issues are also disadvantages when working with microresonator technologies.[57]

The downsizing of magnetoelastic platforms also gives rise to a reduction of the total surface that later on will play a crucial role to host active layers able to detect specific chemical or biological compounds. Hence, the smaller the specific active layers, the smaller the mass change associated with the capture or interaction with the final targets to detect.

As a consequence, alternative strategies to improve the sensitivity avoiding the magnetoelastic resonator size reduction have already been considered, with truly interesting results. In particular, the importance of the magnetoelastic resonator geometry in the mass sensitivity or the resonance quality factor has been duly investigated recently by exploring the magnetoelastic response of triangular and arched triangular-shaped magnetoelastic resonators.[31,103] In comparison to classic rectangular geometries,[40] unconventional triangular and arched triangular resonators exhibit a huge increase in the sensor performance in terms of mass sensitivity and quality of the signal.[31] Particularly, for a similar length of 25 mm, a 4-fold increase in the sensitivity from 1.22 Hz/μg up to 5.34 Hz/μg is obtained when using an arched triangular-shaped magnetoelastic resonator instead of the rectangular classic shapes.

Other resonator geometries have been explored so far. In that context, Saiz et al. recently reported a new geometry based on a rhombic symmetric-shaped resonator that increased by a factor of ~1.53 the resonance frequency with respect to the classic rectangular systems of the same length.[32] A theoretical equation for the resonance frequency of rhombic resonators was obtained, and the experimental and simulations results agree with this theoretical equation. Finally, the higher mass sensitivity of this novel geometry compared with the rectangular one was experimentally demonstrated. Figure 11 summarizes those novel approaches and results obtained by shifting to novel resonator geometries.

By following a similar strategy, Ren et al. recently reported an improvement in the resonance response when resonators

https://doi.org/10.1021/acssensors.2c00032
ACS Sens. XXXX, XXX, XXX−XXX

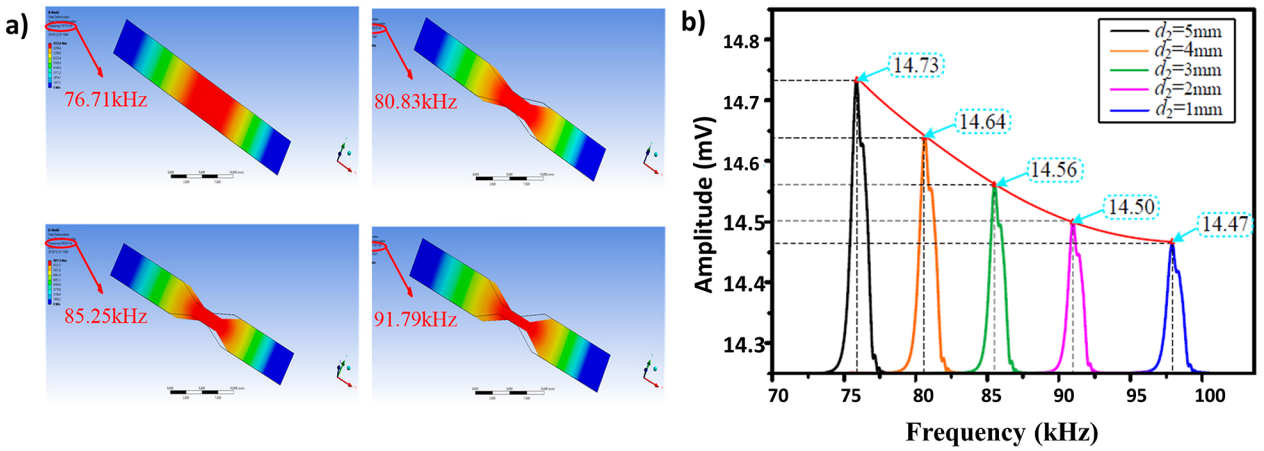

Figure 12. (a) Scheme of the hourglass-shaped magnetoelastic resonator with simulated resonance frequency. (b) Experimental resonance frequencies measured for hourglass-shaped resonators of 30 mm in length with different "neck" sizes. Reproduced with permission from ref 56. Copyright (2020) MDPI.

are shaped as hourglass geometries.[56] An increase in the resonance frequency, which is translated into a mass sensitivity gain, was reported as the neck width of the hourglass geometry was reduced (Figure 12b). This sensitivity increases as hourglass-shaped resonators are ascribed to both the change on the geometry and the reduction of the surface of the nodal position of the resonator (red zone in Figure 12a).

The nodal position of a magnetoelastic resonator is the part of the sensor that does not suffer any displacement during the resonance and, hence, does not contribute to the frequency shift under an external stimulus such as a mass deposition. This is an important characteristic of magnetoelastic resonators, since it means that they have blind points/zones (nodes of vibration), which do not contribute to the sensing process.[104,105] Moreover, the position of these nodes depends on the measurement resonance modes. Figure 13a illustrates the blind measuring points of the first three resonance modes for a rectangular magnetoelastic resonator. As observed in the same figure, the blind points could be overcome by measuring at different resonance modes (Figure 13b).

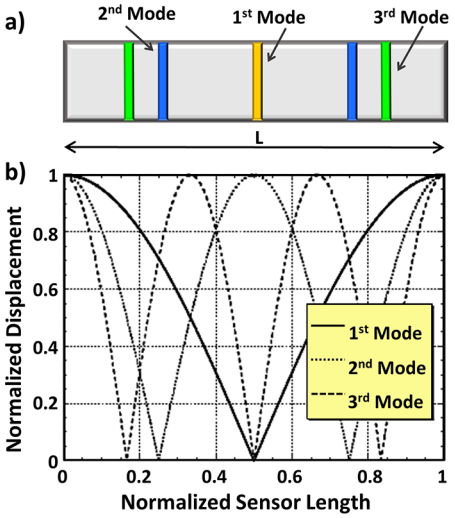

Figure 13. (a) Nodal positions for the first three resonance modes on a rectangular magnetoelastic resonator. (b) Magnitude of the sensor displacement as a function of location for the three lowest resonant modes. Reproduced with permission from ref 105. Copyright (2016) IOP Publishing Ltd.

Partial Loadings: Hot Magnetoelastic Sensing Areas. As opposed to the blind sensing points, there are some areas of the magnetic resonators that exhibit the highest displacement values during resonance (Figure 13b), and hence, they can be defined as hot-sensitive regions of magnetoelastic resonators. In these regions, mass loading leads to a higher frequency shift and hence to a higher mass sensitivity value. Thus, the position of the mass loading strongly influences the resonant frequency shift and, consequently, the sensitivity.

The hot sensing zones within magnetic resonator platforms have already been used to further improve their performance. The effect of mass loading position, asymmetric mass loads, or selective and concurrent measurements in different resonance modes are some of the strategies that have been deeply explored in order to extract the maximum detection capacity of magnetoelastic resonance-based sensors. Ramasamy and Prorok were the first to analyze the effect of mass distribution on the magnetoelastic sensor response by computer simulations.[106] By measuring in the first resonance mode, they observed that a uniform mass distribution led to a linear response of the frequency shift as a function of the mass increase and that the maximum resonance frequency shift for an equal mass increase is obtained when the mass is deposited at the end points of the resonator. Oppositely, a null frequency shift was measured when the mass was deposited at the nodal position. Figure 14a illustrates these findings, showing the resonance frequency shift for a given mass located at different delimited areas of the resonator. Based on these results, Ramasamy and Prorok developed an equation to model the resonator frequency shift as a function of the mass location.[106]

The concept to identify the blind and hot sensing areas within resonators was further developed later on. In particular, Zhang et al. deeply investigated the effect of asymmetric mass loads on magnetoelastic resonator response by means of theoretical calculations.[107] They identified the theoretical resonance frequency shift expected under specific locations of the mass load, as well as the blind point displacement under those asymmetric loadings. This strategy allowed identification of the blind and hot sensitivity areas of the resonator, as illustrated in Figure 14b. Results indicated that when mass is deposited at just one tip of the resonator, the mass sensitivity is

https://doi.org/10.1021/acssensors.2c00032
ACS Sens. XXXX, XXX, XXX−XXX

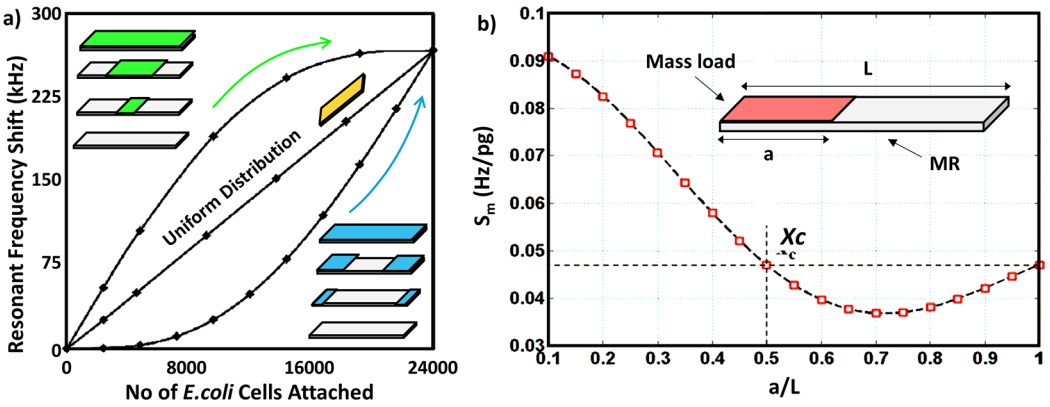

Figure 14. (a) Plots representing the resonant frequency shift of a ME resonator of 250 μm in length under different mass distributions along the resonator.[106] (b) Mass sensitivity (S_m) as a function of the mass distribution length ratio (a/l) for asymmetric mass loadings. Reproduced with permission from ref 107. Copyright (2014) AIP Advances.

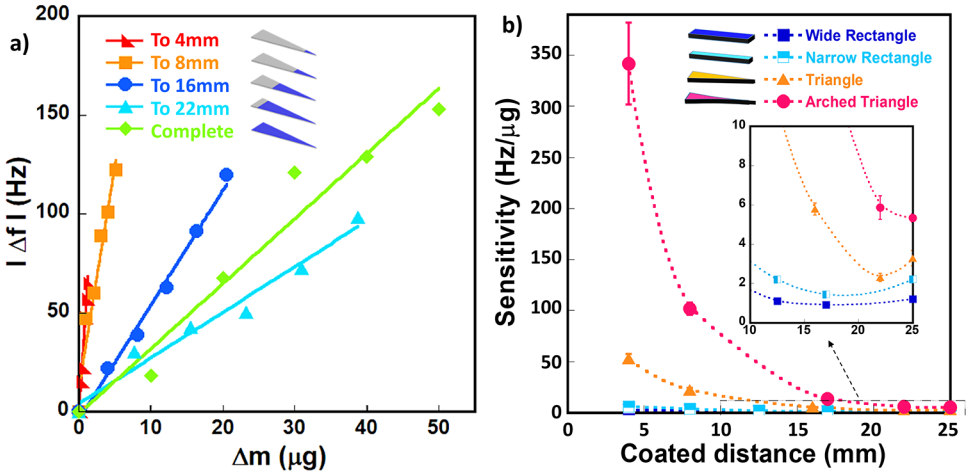

Figure 15. (a) Frequency shift as a function of the deposited mass at different distances from the tip of a triangular Metglas resonator of 25 mm in length. (b) Experimental mass sensitivities as a function of the coated distance measured for different resonator geometries. Inset: Detail of the lowest mass sensitivity response. Reproduced with permission from ref 31. Copyright (2019) Elsevier.

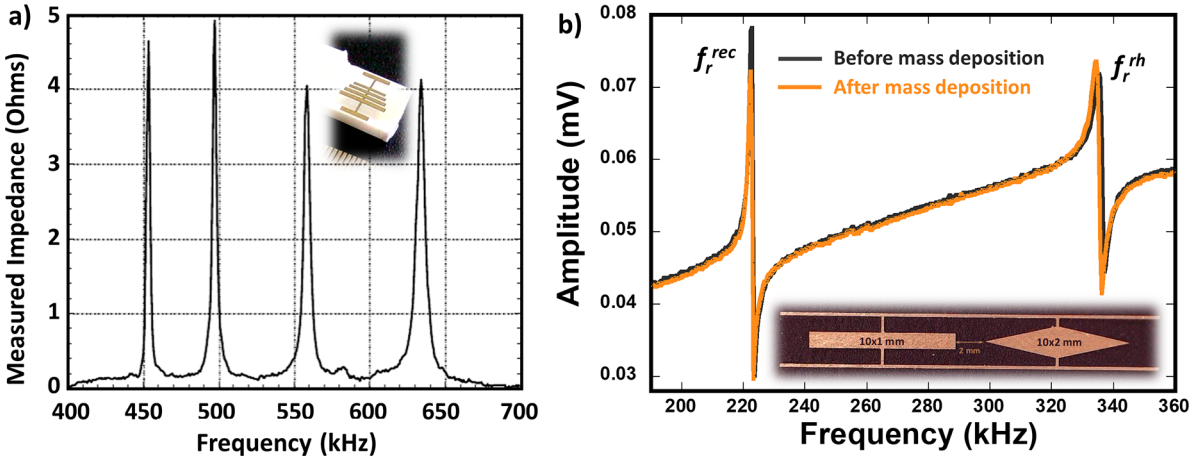

Figure 16. (a) Resonance frequency curves measured for the multisensor with multiple rectangular resonators showed in the image. Reproduced with permission from ref 40. Copyright (2002) MDPI. (b) Resonance frequency curves measured for the multisensor based on the combination of rectangular and rhombic resonators in a single resonator (see inset image). Edited from ref 40. Copyright (2020) IEEE.

maximum at this point, and then it starts to decrease until a point far away from the nodal position, and finally it increases a little again. These asymmetric loads lead therefore to a displacement of the position of the resonator node.

The partial mass loading approach has more recently been expanded to resonators with unconventional geometries, such as the triangle and the arched triangle resonators described in the previous section. This research confirmed that the mass

https://doi.org/10.1021/acssensors.2c00032
ACS Sens. XXXX, XXX, XXX−XXX

sensitivity increases significantly when the mass load is located far from the blind point and close to the tip or tips of the resonator (for the first resonance mode).[31] Results of the frequency shift as a function of the mass load position obtained for the triangular geometry, together with the mass sensitivities obtained for the different geometries, are represented in Figure 15. The position of the node on these novel geometries was also investigated showing that for asymmetric shapes the node is displaced from a position farther away from the tip.

Moreover, as the location of the blind points in the resonator depends on the resonance mode itself, Li and Cheng studied the effect of the mass load location on the resonance frequency shift at different resonance modes.[104] They confirmed that a mass load on the resonator center does not affect the frequency when measuring in the first resonance mode, while the frequency shift was maximum at this point when measuring in the second resonance mode and so on. In a similar way, Zhang et al. analyzed the influence of the mass loading position and resonance mode on the mass sensitivity in a liquid medium, with the aim of investigating the effect of the viscous damping coefficient on the sensitivity.[108] It was found that sensitivity decreases with the increase of the viscous damping coefficient, but this tendency became weaker at higher resonance modes. All these results indicated the clear advantages of ME sensors which, unlike other AW sensors, could overcome the blind point issue by operating under both odd and even modes, which is the direct benefit of its freestanding nature.[41]

Multisensors: Combining Different Nodal Positions and Multiple Resonators. Since the nodal position is dependent on the resonance modes, a single resonator can work as a multisensor depending on the resonance mode measured. In this context, DeRouin and Ong confirmed the feasibility of a single resonator as a multisensor by applying mass loads on the blind points for the different resonance modes (Figure 16a) and measuring later the resonance frequency shift at each resonance mode.[105]

In a similar way, the combination of rectangular resonators with different lengths enables the design of multisensors with different resonance frequencies (Figure 16a).[40,109] This approach has been already applied for real sensing of biological compounds.

Most recently, a multiple sensor design based on the combination of resonators with different geometries (rectangle + rhombic resonators) of the same length has been developed.[32] Each resonator present a different resonance frequency peak that can be simultaneously measured to detect in a concurrent mode different target chemicals. Unlike for multiresonators exhibiting ribbons with the same geometry but different sizes, in this case the surface area associated with each resonator is the same, which can be an advantage for comparative purposes (Figure 16b).

Overall, multisensor technology based on single or multiple magnetoelastic resonators is in a nascent stage, but it holds great potential to incorporate in the same device specific sites to monitor and/or concurrently capture physicochemical parameters or target analytes of varied natures.

CONCLUSIONS AND FUTURE PERSPECTIVES

Magnetoelastic sensors are among the most appealing transducers, since they are able to measure and sense a varied scope of physical, chemical, and biological targets in a continuous, concurrent, and wireless mode. These characteristics, together with their outstanding sensitivity, make a difference in comparison to alternative technologies to achieve continuous and reliable monitoring of industrial, environmental, and biological processes, among others. In addition, their wireless sensing response make ME sensors perfectly fit into the Internet of things (IoT) and the future industrial and environmental digitalization aims.

Over the last years, magnetoelastic sensors have been employed for the in situ detection of microorganisms, air and water pollutants, or physical parameters such as viscosity or density of complex fluids such as blood. Notwithstanding their impressive performances, there is still room for improvement to further tune the selectivity and sensitivity of magnetoelastic ribbons on the road to a mature technology.

While the detection of viscosity or density changes can be directely measured by a bare resonator, different materials have been used to functionalize their surface and so improve their selectivity to sense specific chemical or biological targets. The variety of active layers employed to functionalize magnetoelastic ribbons reflects the tremendous versatility of this technology. From antibodies and zeolites to the recently employed bacteriophages and metal−organic frameworks (for biological and chemical detection, repectively), a variety of options are available to encode the surface of the magnetic resonators.

The perspective to increase the sensitivity of magnetoelastic resonators by modifying their geometry, applying partial coatings, or microsizing the ME ribbons through advanced manufacturing will be key aspects to improve ME sensor performance and hence to extend the range of applications accessible for this technological platform. Moreover, recent developments in magnetoelastic sensors for simultaneous multiparameter monitoring could further expand the potentials of magnetoelastic transducers. Selective mass loadings at blind resonance areas of different resonance modes or the combination of varied geometries in a single resonator will open the propects for further improvement and expansion, both on the base ground research to understand the magnetoelastic resonators performance and on their advanced application in ultralow multidetection purposes.

AUTHOR INFORMATION

Corresponding Author

Paula G. Saiz − *BCMaterials, Basque Center for Materials, Applications and Nanostructures, 48940 Leioa, Spain; Department of Geology, Science and Technology Faculty, University of the Basque Country (UPV/EHU), 48940 Leioa, Spain;* orcid.org/0000-0003-1775-8486; Email: paula.gonzalez@bcmaterials.net

Authors

Roberto Fernández de Luis − *BCMaterials, Basque Center for Materials, Applications and Nanostructures, 48940 Leioa, Spain;* orcid.org/0000-0002-8924-230X

Andoni Lasheras − *Department of Physics, Science and Technology Faculty, University of the Basque Country (UPV/EHU), 48940 Leioa, Spain;* orcid.org/0000-0003-2738-2267

María Isabel Arriortua − *BCMaterials, Basque Center for Materials, Applications and Nanostructures, 48940 Leioa, Spain; Department of Geology, Science and Technology Faculty, University of the Basque Country (UPV/EHU), 48940 Leioa, Spain*

https://doi.org/10.1021/acssensors.2c00032
ACS Sens. XXXX, XXX, XXX−XXX

Ana Catarina Lopes − *Grupo de Química Macromolecular, Departamento Química-Física, Universidad del País Vasco, UPV-EHU, 48940 Vizcaya, Spain; Centre for Cooperative Research on Alternative Energies (CIC energiGUNE), Basque Research and Technology Alliance (BRTA), 01510 Vitoria-Gasteiz, Spain; IKERBASQUE, Basque Foundation for Science, 48009 Bilbao, Spain*

Complete contact information is available at: https://pubs.acs.org/10.1021/acssensors.2c00032

Author Contributions

The manuscript was written through contributions of all authors and all authors reviewed and approved the final version.

Notes

The authors declare no competing financial interest.

■ ACKNOWLEDGMENTS

The authors thank the support from the "Ministerio de Economía, Industria y Competitividad" (MAT2016-76739-R (AEI/FEDER, UE)) and from the European Commission Research & Innovation under the H2020-MSCA-RISE-2017 (ref.: 778412 INDESMOF project).

■ ABBREVIATIONS

CDNA, complementary DNA; CEA, carcinoembryonic antigen; CNC, computer numerical control; HMs, heavy metals; HSA, human serum albumin; IoT, Internet of Things; ME, magnetoelastic; MOF, metal organic framework; PBS, phosphate buffered saline; SEM, scanning electron microscopy; VOCs, volatile organic compounds

■ VOCABULARY

Magnetoelastic sensor, a cheap and wireless technology for sensing; magnetoelastic coupling: effective energy interchange from magnetic to elastic and viceversa; magnetostrictive effect, relative deformation suffered by a ferromagnetic material subjected to an external magnetic field; magnetoelastic effect, change in the magnetic state of a ferromagnetic material subjected to a mechanical stress

■ REFERENCES

(1) Sinclair, I. *Sensors and transducers*; Elsevier, 2000.
(2) Sharapov, V.; Sotula, Z.; Kunickaya, L. *Piezo-electric electro-acoustic transducers*; Springer International Publishing, 2014.
(3) Felix, F. S.; Angnes, L. Electrochemical immunosensors−a powerful tool for analytical applications. *Biosens. Bioelectron.* **2018**, *102*, 470−478.
(4) Nakamura, K. *Ultrasonic transducers: Materials and design for sensors, actuators and medical applications*; Elsevier, 2012.
(5) Alaba, F. A.; Othman, M.; Hashem, I. A. T.; Alotaibi, F. Internet of Things security : A survey. *J. Network Comput. Appl.* **2017**, *88*, 10−28.
(6) Morello, R.; Mukhopadhyay, S. C.; Liu, Z.; Slomovitz, D.; Samantaray, S. R. Advances on sensing technologies for smart cities and power grids: A review. *IEEE Sensors Journal* **2017**, *17*, 7596−7610.
(7) Tong, A.; Sorrell, T. C.; Black, A. J.; Caillaud, C.; Chrzanowski, W.; Li, E.; Martinez-Martin, D.; McEwan, A.; Wang, R.; Motion, A.; Casas Bedoya, A.; Huang, J.; Azizi, L.; Eggleton, B. J. Research priorities for COVID-19 sensor technology. *Nat. Biotechnol.* **2021**, *39*, 144−147.
(8) Kassal, P.; Steinberg, M. D.; Steinberg, I. M. Wireless chemical sensors and biosensors: A review. *Sensors Actuators, B Chem.* **2018**, *266*, 228−245.
(9) Pulugu, P.; Ghosh, S.; Rokade, S.; Choudhury, K.; Arya, N.; Kumar, P. A perspective on implantable biomedical materials and devices for diagnostic applications. *Curr. Opin. Biomed. Eng.* **2021**, *18*, 100287.
(10) Huang, S.; Yang, H.; Lakshmanan, R. S.; Johnson, M. L.; Wan, J.; Chen, I.; Wikle, H. C., III; Petrenko, V. A.; Barbaree, J. M.; Chin, B. A. Sequential detection of Salmonella typhimurium and Bacillus anthracis spores using magnetoelastic biosensors. *Biosens. Bioelectron.* **2009**, *24*, 1730−1736.
(11) Guo, X.; Sang, S.; Jian, A.; Gao, S.; Duan, Q.; Ji, J.; Zhang, Q.; Zhang, W. A bovine serum albumin-coated magnetoelastic biosensor for the wireless detection of heavy metal ions. *Sensors Actuators. B Chem.* **2018**, *256*, 318−324.
(12) Campanile, R.; Scardapane, E.; Forente, A.; Granata, C.; Germano, R.; Di Girolamo, R.; Minopoli, A.; Velota, R.; Della Ventura, B.; Iannotti, V. Core-shell magnetic nanoparticles for highly sensitive magnetoelastic immunosensor. *Nanomaterials* **2020**, *10*, 1526.
(13) Lim, H. J.; Saha, T.; Tey, B. T.; Tan, W. S.; Ooi, C. W. Quartz crystal microbalance-based biosensors as rapid diagnostic devices for infectious diseases. *Biosens. Bioelectron.* **2020**, *168*, 112513.
(14) Mouro, J.; Pinto, R.; Paoletti, P.; Tiribilli, B. Microcantilever: Dynamical response for mass sensing and fluid characterization. *Sensors* **2021**, *21*, 115.
(15) Devkota, J.; Ohodnicki, P. R.; Greve, D. W. SAW sensors for chemical vapors and gases. *Sensors* **2017**, *17*, 801.
(16) Stoyanov, P. G.; Grimes, C. A. A remote query magnetostrictive viscosity sensor. *Sensors Actuators, A Phys.* **2000**, *80*, 8−14.
(17) Grimes, C. A.; Kouzoudis, D.; Mungle, C. Simultaneous measurement of liquid density and viscosity using remote query magnetoelastic sensors. *Rev. Sci. Instrum.* **2000**, *71*, 3822.
(18) Mungle, C.; Grimes, C. A.; Dreschel, W. R. Magnetic field tuning of the frequency-temperature response of a magnetoelastic sensor. *Sensors Actuators, A Phys.* **2002**, *101*, 143−149.
(19) Kouzoudis, D.; Grimes, C. A. The frequency response of magnetoelastic sensors to stress and atmospheric pressure. *Smart Mater. Struct.* **2000**, *9*, 885−889.
(20) Ruan, C.; Zeng, K.; Grimes, C. A. A mass-sensitive pH sensor based on a stimuli-responsive polymer. *Anal. Chim. Acta* **2003**, *497*, 123−131.
(21) Atalay, S.; Izgi, T.; Kolat, V. S.; Erdemoglu, S.; Inan, O. O. Magnetoelastic humidity sensors with TiO2 nanotube sensing layers. *Sensors* **2020**, *20*, 425.
(22) Baimpos, T.; Boutikos, P.; Nikolakis, V.; Kouzoudis, D. A polymer-Metglas sensor used to detect volatile organic compounds. *Sensors Actuators, A Phys.* **2010**, *158*, 249−253.
(23) Huang, Y. Q.; Yin, J. C.; Wang, Y. S.; Xiao, X. L.; Zhou, B.; Xue, J. H.; Tang, X.; Wang, X. F.; Zhu, Y. F.; Chen, S. H. Streptavidin and gold nanoparticles-based dual signal amplification for sensitive magnetoelastic sensing of mercury using a specific aptamer probe. *Sensors Actuators, B Chem.* **2016**, *235*, 507−514.
(24) Guo, X.; Sang, S.; Guo, J.; Jian, A.; Duan, Q.; Ji, J.; Zhang, Q.; Zhang, W. A magnetoelastic biosensor based on E2 glycoprotein for wireless detection of classical swine fever virus E2 antibody. *Sci. Rep.* **2017**, *7*, 1−8.
(25) Beltrami, L. V. R.; Beltrami, M.; Roesch-Ely, M.; Kunst, S. R.; Missell, F. P.; Birriel, E. J.; de F. Malfatti, C. Magnetoelastic sensors with hybrid films for bacteria detection in milk. *J. Food Eng.* **2017**, *212*, 18−28.
(26) Le Bras, Y.; Greneche, J. M. Magnetoelastic resonance: Principles, modeling and applications. *Resonance* **2017**, *2*, 13−34.
(27) Hristoforou, E. Magnetostrictive delay lines: engineering theory and sensing applications. *Meas. Sci. Technol.* **2003**, *14*, R15.
(28) Bravo, I.; Arnaiz, A.; Garcia-Arribas, A. Damping of magnetoelastic resonance for oil viscosity sensing. *IEEE Trans. Magn.* **2019**, *55*, 1.

(29) Cheng, P.; Gao, S.; Zhang, W.; Wang, T.; Jian, A.; Sang, S. Resonance modes of freestanding magnetoelastic resonator and the application in viscosity measurement. *Smart Mater. Struct.* **2015**, *24*, 045029.
(30) Zhang, K.; Zhang, L.; Chai, Y. Mass load distribution dependence of mass sensitivity of magnetoelastic sensors under different resonance modes. *Sensors* **2015**, *15*, 20267−20278.
(31) Saiz, P. G.; Gandia, D.; Lasheras, A.; Sagasti, A.; Quintana, I.; Fdez-Gubieda, M. L.; Gutiérrez, J.; Arriortua, M. I.; Lopes, A. C. Enhanced mass sensitivity in novel magnetoelastic resonators geometries for advanced detection systems. *Sensors Actuators, B Chem.* **2019**, *296*, 126612.
(32) Saiz, P. G.; Gutierrez, J.; Arriortua, M. I.; Lopes, A. C. Theoretical and experimental analysis of novel rhombus shaped magnetoelastic sensors with enhanced mass sensitivity. *IEEE Sensors* **2020**, *20*, 13332−13340.
(33) Sagasti, A.; Gutierrez, J.; San Sebastian, M.; Barandiaran, J. M. Magnetoelastic resonators for highly specific chemical and biological detection: A critical study. *IEEE Trans. Magn.* **2017**, *53*, 1.
(34) Johnson, M. L.; Wan, J.; Huang, S.; Cheng, Z.; Petrenko, V. A.; Kim, D.-J.; Chen, I.-H.; Barbaree, J. M.; Hong, J. W.; Chin, B. A. A wireless biosensor using microfabricated phage-interfaced magnetoelastic particles. *Sensors Actuators, A Phys.* **2008**, *144*, 38−47.
(35) Landau, L. D.; Lifshitz, E. M. *Theory of Elasticity*; Pergamon: Oxford, 1986; Chapter II.
(36) Kabacoff, L. T.; Wun-Fogle, M. Magnetomechanical properties of flash annealed Metglas 2605 SC. *J. Appl. Phys.* **1985**, *57*, 3499.
(37) Sagasti, A.; Gutiérrez, J.; Lasheras, A.; Barandiarán, J. M. Size dependence of the magnetoelastic properties of metallic glasses for actuation applications. *Sensors* **2019**, *19*, 4296.
(38) Petersan, P. J.; Anlage, S. M. Measurement of resonant frequency and quality factor of microwave resonators: Comparison of methods. *J. Appl. Phys.* **1998**, *84*, 3392−3402.
(39) Lopes, A. C.; Sagasti, A.; Lasheras, A.; Muto, V.; Gutierrez, J.; Kouzoudis, D.; Barandiaran, J. M. Accurate determination of the Q quality factor in magnetoelastic resonant platforms for advanced biological detection. *Sensors* **2018**, *18*, 887.
(40) Grimes, C. A.; Roy, S. C.; Rani, S.; Cai, Q. Theory, instrumentation and applications of magnetoelastic resonance sensors: A review. *Sensors* **2011**, *11*, 2809−2844.
(41) Zhang, K.; Zhang, L.; Fu, L.; Li, S.; Chen, H.; Cheng, Z. Y. Magnetostrictive resonators as sensors and actuators. *Sensors Actuators, A Phys.* **2013**, *200*, 2−10.
(42) Hernando, A.; Vazquez, M.; Barandiaran, J. M. Metallic glasses and sensing applications. *J. Phys. E* **1988**, *21*, 1129−1139.
(43) Ren, L.; Yu, K.; Tan, Y. Applications and advances of magnetoelastic sensors in biomedical engineering: A review. *Materials (Basel)* **2019**, *12*, 1135.
(44) Li, S.; Horikawa, S.; Park, M.-k.; Chai, Y.; Vodyanoy, V. J.; Chin, B. A. Amorphous metallic glass biosensors. *Intermetallics* **2012**, *30*, 80−85.
(45) Metglas Safety Data Sheet (October 2021). https://metglas.com/wp-content/uploads/2016/12/Metglas-Alloy-2605HB1-Iron-Based-Alloy-also-for-2605HB1M.pdf.
(46) Metglas (October 2021). www.metglas.com, https://metglas.com/wp-content/uploads/2016/12/2826MB-Technical-Bulletin.pdf.
(47) Atalay, S.; Kolat, V. S.; Atalay, F. E.; Bayri, N.; Kaya, H.; Izgi, T. Magnetoelastic sensor for magnetic nanoparticle detection. *J. Magn. Magn. Mater.* **2018**, *465*, 151−155.
(48) Atalay, S.; Kolat, V. S.; Bayri, N.; Izgi, T. Magnetoelastic sensor studies on amorphous magnetic FeSiB wire and the application in viscosity measurement. *J. Supercond. Nov. Magn.* **2016**, *29*, 1551.
(49) Johnson, M. L.; LeVar, O.; Yoon, S. H.; Park, J. H.; Huang, S.; Kim, D. J.; Cheng, Z.; Chin, B. A. Dual-cathode method for sputtering magnetoelastic iron-boron films. *Vacuum* **2009**, *83*, 958−964.
(50) Sang, S.; Cheng, P.; Zhang, W.; Li, P.; Hu, J.; Li, G.; Jian, A. Investigation on a new Fe83Ga17 wire-based magnetoelastic resonance biosensor. *J. Intell. Mater. Syst. Struct.* **2015**, *26*, 980−987.
(51) Thomas, S.; Mathew, J.; Radhakrishnan, P.; Nampoori, V. P. N.; George, A. K.; Al-Harthi, S. H.; Ramanujan, R. V.; Anantharaman, M. R. Metglas thin film based magnetostrictive transducers for use in long period fibre grating sensors. *Sensors Actuators, A Phys.* **2010**, *161*, 83−90.
(52) Thang, P. D.; Duong, H. H.; Nghi, N. H. Magnetic and sensitive magnetoelastic properties of Finemet nanostructured ribbon. *J. Phys. Conf. Ser.* **2009**, *187*, 012062.
(53) Atalay, S.; Kaya, H.; Atalay, F. E.; Izgi, T.; Kolat, V. S. Formation and detection of magnetic CoNiFe nanowire network using magnetoelastic sensor. *J. Supercond. Nov. Magn.* **2019**, *32*, 3907−3913.
(54) K. Turunen, M. P.; Herola, E.; Kivilahti, J. K. A wireless biosensing device. *ESTC 2006 - 1st Electron. Syst. Technol. Conf.* **2006**, *2*, 1224−1229.
(55) Huang, S.; Hu, J.; Wan, J.; Johnson, M. L.; Shu, H.; Chin, B. A. The effect of annealing and gold deposition on the performance of magnetoelastic biosensors. *Mater. Sci. Eng., C* **2008**, *28*, 380−386.
(56) Ren, L.; Cong, M.; Tan, Y. An hourglass-shaped wireless and passive magnetoelastic sensor with an improved frequency sensitivity for remote strain measurements. *Sensors* **2020**, *20*, 359.
(57) Johnson, M. L.; Wan, J.; Huang, S.; Cheng, Z.; Petrenko, V. A.; Kim, D.-J.; Chen, I.-H.; Barbaree, J. M.; Hong, J. W.; Chin, B. A. A wireless biosensor using microfabricated phage-interfaced magnetoelastic particles. *Sensors Actuators, A: Phys.* **2008**, *144*, 38−47.
(58) Dalponte, A.; Bastos, E. S.; Missell, F. P. Enhanced response from field-annealed magnetoelastic strain sensor. *J. Appl. Phys.* **2016**, *120*, 064502.
(59) Na, S. M.; Flatau, A. B. Global Goss grain growth and grain boundary characteristics in magnetostrictive Galfenol sheets. *Smart Mater. Struct.* **2013**, *22* (12), 125026.
(60) Holmes, H. R.; Derouin, A.; Wright, S.; Riedemann, T. M.; Lograsso, T. A.; Rajachar, R. M.; Ghee Ong, K. Biodegradation and biocompatibility of mechanically active magnetoelastic materials. *Smart Mater. Struct.* **2014**, *23*, 095036.
(61) Sagasti, A.; Lopes, A. C.; Lasheras, A.; Palomares, V.; Carrizo, J.; Gutierrez, J.; Barandiaran, J. M. Corrosion resistant metallic glasses for biosensing applications. *AIP Adv.* **2018**, *8*, 047702.
(62) Sagasti, A.; Palomares, V.; Porro, J. M.; Orúe, I.; Sánchez-Ilárduya, M. B.; Lopes, A. C.; Gutiérrez, J. Magnetic, magnetoelastic and corrosion resistant properties of (Fe-Ni)-based metallic glasses for structural health monitoring applications. *Materials (Basel)* **2020**, *13*, 57.
(63) Bouropoulos, N.; Kouzoudis, D.; Grimes, C. The real-time, in situ monitoring of calcium oxalate and brushite precipitation using magnetoelastic sensors. *Sensors Actuators, B Chem.* **2005**, *109*, 227−232.
(64) Gao, X.; Yang, W.; Pang, P.; Liao, S.; Cai, Q.; Zeng, K.; Grimes, C. A. A wireless magnetoelastic biosensor for rapid detection of glucose concentrations in urine samples. *Sensors Actuators, B Chem.* **2007**, *128*, 161−167.
(65) Marín, P.; Marcos, M.; Hernando, A. High magnetomechanical coupling on magnetic microwire for sensors with biological applications. *Appl. Phys. Lett.* **2010**, *96*, 262512.
(66) Chen, P.; Jiang, Q.; Horikawa, S.; Li, S. Magnetoelastic-sensor integrated microfluidic chip for the measurement of blood plasma viscosity. *J. Electrochem. Soc.* **2017**, *164*, B247−B252.
(67) Cai, Q. Y.; Cammers-goodwin, A.; Grimes, C. A. A wireless, remote query magnetoelastic CO2 sensor. *J. Environ. Monit.* **2000**, *2*, 556−560.
(68) Cai, Q. Y.; Jain, M. K.; Grimes, C. A. A wireless, remote query ammonia sensor. *Sensors Actuators, B Chem.* **2001**, *77*, 614−619.
(69) Zhang, R.; Tejedor, M. I.; Anderson, M. A.; Paulose, M.; Grimes, C. A. Ethylene detection using nanoporous PtTiO2 coatings applied to magnetoelastic thick films. *Sensors* **2002**, *2*, 331−338.
(70) Giannakopoulos, I. G.; Kouzoudis, D.; Grimes, C. A.; Nikolakis, V. Synthesis and characterization of a composite zeolite-metglas carbon dioxide sensor. *Adv. Funct. Mater.* **2005**, *15*, 1165−1170.

https://doi.org/10.1021/acssensors.2c00032
ACS Sens. XXXX, XXX, XXX−XXX

(71) Baimpos, T.; Gora, L.; Nikolakis, V.; Kouzoudis, D. Selective detection of hazardous VOCs using zeolite/Metglas composite sensors. *Sensors Actuators, A Phys.* **2012**, *186*, 21−31.
(72) G. Saiz, P.; Fernandez de Luis, R.; Bartolome, L.; Gutierrez, J.; Arriortua, M. I.; Lopes, A. C. Rhombic-magnetoelastic/metal-organic framework functionalized resonators for highly sensitive toluene detection. *J. Mater. Chem. C* **2020**, *8*, 13743−13753.
(73) Saiz, P. G.; Porro, J. M.; Lasheras, A.; Fernandez de Luis, R.; Quintana, I.; Arriortua, M. I.; Lopes, A. C. Influence of the magnetic domain structure in the mass sensitivity of magnetoelastic sensors with different geometries. *J. Alloys Compd.* **2021**, *863*, 158555.
(74) Zhao, Z.; Liao, L.; Xiao, X.; Du, N.; Lin, Y. Wireless sensing determination of uranium(IV) based on its inhibitory effect on a catalytic precipitation reaction. *J. Radioanal. Nucl. Chem.* **2011**, *289*, 893−898.
(75) Zhao, Z.; Liao, L.; Xiao, X.; Du, N.; Lin, Y. Determination of uranium in water based on enzyme inhibition using a wireless magnetoelastic sensor. *Int. J. Environ. Anal. Chem.* **2013**, *93*, 613−622.
(76) Sang, S.; Gao, S.; Guo, X.; Cheng, P.; Zhang, W. The detection of Pb2+ in solution using bare magnetoelastic resonator. *Appl. Phys. Lett.* **2016**, *108*, 054102.
(77) Sisniega, B.; Sedano, A. S.; Gutiérrez, J.; García-Arribas, A. Real time monitoring of calcium oxalate precipitation reaction by using corrosion resistant magnetoelastic resonance sensors. *Sensors (Switzerland)* **2020**, *20*, 2802.
(78) Zhang, Z.; Pinnaratip, R.; Ong, K. G.; Lee, B. P. Correlating the mass and mechanical property changes during the degradation of PEG-based adhesive. *J. Appl. Polym. Sci.* **2020**, *137*, 48451.
(79) Sang, S.; Wang, Y.; Feng, Q.; Wei, Y.; Ji, J.; Zhang, W. Progress of new label-free techniques for biosensors: A review. *Crit. Rev. Biotechnol.* **2016**, *36*, 465−481.
(80) Ruan, C.; Zeng, K.; Varghese, O. K.; Grimes, C. A. Magnetoelastic immunosensors: Amplified mass immunosorbent assay for detection of Escherichia coli O157:H7. *Anal. Chem.* **2003**, *75*, 6494−6498.
(81) Zhang, K.; Fu, L.; Zhang, L.; Cheng, Z.; Huang, T. Magnetostrictive particle based biosensors for in situ and real-time detection of pathogens in water. *Biotechnol. Bioeng.* **2014**, *111*, 2229−2238.
(82) Ruan, C.; Zeng, K.; Varghese, O. K.; Grimes, C. A. A staphylococcal enterotoxin B magnetoelastic immunosensor. *Biosens. Bioelectron.* **2004**, *20*, 585−591.
(83) Guntupalli, R.; Hu, J.; Lakshmanan, R. S.; Huang, T.S.; Barbaree, J. M.; Chin, B. A. A magnetoelastic resonance biosensor immobilized with polyclonal antibody for the detection of Salmonella typhimurium. *Biosens. Bioelectron.* **2007**, *22*, 1474−1479.
(84) Lakshmanan, R. S.; Guntupalli, R.; Hu, J.; Petrenko, V. A.; Barbaree, J. M.; Chin, B. A. Detection of Salmonella typhimurium in fat free milk using a phage immobilized magnetoelastic sensor. *Sensors Actuators, B Chem.* **2007**, *126*, 544−550.
(85) Li, S.; Li, Y.; Chen, H.; Horikawa, S.; Shen, W.; Simonian, A.; Chin, B. A. Direct detection of Salmonella typhimurium on fresh produce using phage-based magnetoelastic biosensors. *Biosens. Bioelectron.* **2010**, *26*, 1313−1319.
(86) Chai, Y.; Li, S.; Horikawa, S.; Park, M. K.; Vodyanoy, V.; Chin, B. A. Rapid and sensitive detection of salmonella typhimurium on eggshells by using wireless biosensors. *J. Food Prot.* **2012**, *75*, 631−636.
(87) Wang, F.; Horikawa, S.; Hu, J.; Wikle, H. C.; Chen, I. H.; Du, S.; Liu, Y.; Chin, B. A. Detection of Salmonella typhimurium on spinach using phage-based magnetoelastic biosensors. *Sensors* **2017**, *17*, 386.
(88) Guo, X.; Wang, J.; Zhao, Y.; Liu, R.; Zhang, Q.; Yuan, Z.; Sang, S. A wireless magnetoelastic DNA-biosensor amplified by AuNPs for the detection of a common mutated DNA causing β-thalassaemia. *Biochem. Eng. J.* **2020**, *156*, 107498.
(89) Sang, S.; Guo, X.; Wang, J.; Li, H.; Ma, X. Real-time and label-free detection of: VKORC1 genes based on a magnetoelastic biosensor for warfarin therapy. *J. Mater. Chem. B* **2020**, *8*, 6271−6276.
(90) Huang, X.; Sang, S.; Yuan, Z.; Duan, Q.; Guo, X.; Zhang, H.; Zhao, C. Magnetoelastic Immunosensor via Antibody Immobilization for the Specific Detection of Lysozymes. *ACS Sensors* **2021**, *6*, 3933−3939.
(91) Liu, R.; Guo, X.; Wang, J.; Guo, J.; Zhang, Y.; Zhang, W.; Sang, S. High sensitivity detection of human serum albumin using a novel magnetoelastic immunosensor. *J. Mater. Sci.* **2019**, *54*, 9679−9688.
(92) Wang, J.; Guo, X.; Liu, R.; Guo, J.; Zhang, Y.; Zhang, W.; Sang, S. Detection of carcinoembryonic antigen using a magnetoelastic nano-biosensor amplified with DNA-templated silver nanoclusters. *Nanotechnology* **2020**, *31*, 015501.
(93) Sagasti, A.; Bouropoulos, N.; Kouzoudis, D.; Panagiotopoulos, A.; Topoglidis, E.; Gutiérrez, J. Nanostructured ZnO in a Metglas/ZnO/hemoglobin modified electrode to detect the oxidation of the hemoglobin simultaneously by cyclic voltammetry and magnetoelastic resonance. *Materials (Basel)* **2017**, *10*, 849.
(94) Shekhar, S.; Karipott, S. S.; Guldberg, R. E.; Ong, K. G. Magnetoelastic sensors for real-time tracking of cell growth. *Biotechnol. Bioeng.* **2021**, *118*, 2380−2385.
(95) Menti, C.; Beltrami, M.; Possan, A. L.; Martins, S. T.; Henriques, J. A.P.; Santos, A. D.; Missell, F. P.; Roesch-Ely, M. Biocompatibility and degradation of gold-covered magneto-elastic biosensors exposed to cell culture. *Colloids Surfaces B Biointerfaces* **2016**, *143*, 111−117.
(96) Shen, W.; Lakshmanan, R. S.; Mathison, L. C.; Petrenko, V. A.; Chin, B. A. Phage coated magnetoelastic micro-biosensors for real-time detection of Bacillus anthracis spores. *Sensors Actuators, B Chem.* **2009**, *137*, 501−506.
(97) Xue, C.; Yang, C.; Xu, T.; Zhan, J.; Li, X. A wireless bio-sensing microfluidic chip based on resonating 'μ-divers. *Lab Chip* **2015**, *15*, 2318−2326.
(98) Possan, A. L.; Menti, C.; Beltrami, M.; Santos, A. D.; Roesch-Ely, M.; Missell, F. P. Effect of surface roughness on performance of magnetoelastic biosensors for the detection of Escherichia coli. *Mater. Sci. Eng., C* **2016**, *58*, 541−547.
(99) Sang, S.; Guo, X.; Liu, R.; Wang, J.; Guo, J.; Zhang, Y.; Yuan, Z.; Zhang, W. A novel magnetoelastic nanobiosensor for highly sensitive detection of atrazine. *Nanoscale Res. Lett.* **2018**, *13*, 1 DOI: 10.1186/s11671-018-2840-7.
(100) Karipott, S. S.; Fear, K.; Nelson, B.; Leguineche, K.; Lin, A.; Shekhar, S.; Guldberg, R. E.; Ong, K. G. A magnetoelastic bone fixation device for controlled mechanical stimulation at femoral fractures in rodents. *Eng. Res. Express* **2021**, *3*, 035028.
(101) Menti, C.; Henriques, J. A. P.; Missell, F. P.; Roesch-Ely, M. Antibody-based magnetoelastic biosensors: potential devices for detection of pathogens and associated toxins. *Appl. Microbiol. Biotechnol.* **2016**, *100*, 6149−6163.
(102) Shen, W.; Mathison, L. C.; Petrenko, V. A.; Chin, B. A. Design and characterization of a magnetoelastic sensor for the detection of biological agents. *J. Phys. D. Appl. Phys.* **2010**, *43*, 015004.
(103) Pacella, N.; Derouin, A.; Pereles, B.; Ong, K. G. Geometrical modification of magnetoelastic sensors to enhance sensitivity. *Smart Mater. Struct.* **2015**, *24*, 025018.
(104) Li, S.; Cheng, Z. Y. Nonuniform mass detection using magnetostrictive biosensors operating under multiple harmonic resonance modes. *J. Appl. Phys.* **2010**, *107*, 114514.
(105) DeRouin, A.; Ong, K. G. Multi-parameter sensing with a single magnetoelastic sensor by applying loads on the null locations of multiple resonant modes. *Smart Mater. Struct.* **2016**, *25*, 035044.
(106) Ramasamy, M.; Prorok, B. C. Resonance behavior of magnetostrictive sensor in biological agent detection. *IMECE201* **2010**, 1−7.
(107) Zhang, K.; Zhang, K.; Chai, Y. Study of 'blind point' and mass sensitivity of a magnetostrictive biosensor with asymmetric mass loading. *AIP Adv.* **2014**, *4*, 057114.
(108) Zhang, K.; et al. Damping force and loading position dependence of mass sensitivity of magnetoelastic biosensors in viscous liquid. *Sensors* **2019**, *19*, 1−9.

https://doi.org/10.1021/acssensors.2c00032
ACS Sens. XXXX, XXX, XXX−XXX

(109) Grimes, C. A.; Mungle, C. S.; Zeng, K.; Jain, M. K.; Dreschel, W. R.; Paulose, M.; Ong, K. G. Wireless magnetoelastic resonance sensors: A critical review. *Sensors* **2002**, *2*, 294−313.

https://doi.org/10.1021/acssensors.2c00032
ACS Sens. XXXX, XXX, XXX−XXX